BJ www.biochemj.org

BJ Metabolism

Biochem. J. (2012) **443**, 535–547 (Printed in Great Britain) doi:10.1042/BJ20111478

online data

Novel structural arrangement of nematode cystathionine β-synthases: characterization of *Caenorhabditis elegans* CBS-1

Roman VOZDEK, Aleš HNÍZDA, Jakub KRIJT, Marta KOSTROUCHOVÁ and Viktor KOŽICH[1]

Institute of Inherited Metabolic Disorders, Charles University in Prague, First Faculty of Medicine and General University Hospital, Ke Karlovu 2, 128 08, Praha 2, Czech Republic

CBSs (cystathionine β-synthases) are eukaryotic PLP (pyridoxal 5 *-phosphate)-dependent proteins that maintain cellular homocysteine homoeostasis and produce cystathionine and hydrogen sulfide. In the present study, we describe a novel structural arrangement of the CBS enzyme encoded by the *cbs-1* gene of the nematode *Caenorhabditis elegans*. The CBS-1 protein contains a unique tandem repeat of two evolutionarily conserved catalytic regions in a single polypeptide chain. These repeats include a catalytically active C-terminal module containing a PLP-binding site and a less conserved N-terminal module that is unable to bind the PLP cofactor and cannot catalyse CBS reactions, as demonstrated by analysis of truncated variants and active-site mutant proteins. In contrast with other metazoan enzymes, CBS-1 lacks the haem and regulatory Bateman domain essential for activation by AdoMet (*S*-adenosylmethionine) and only forms monomers. We determined the tissue and subcellular distribution of CBS-1 and showed that *cbs-1* knockdown by RNA interference leads to delayed development and to an approximately 10-fold elevation of homocysteine concentrations in nematode extracts. The present study provides the first insight into the metabolism of sulfur amino acids and hydrogen sulfide in *C. elegans* and shows that nematode CBSs possess a structural feature that is unique among CBS proteins.

Key words: cystathionine β-synthase (CBS), *Caenorhabditis elegans*, domain architecture, homocysteine, hydrogen sulfide, knockdown.

INTRODUCTION

Methionine and cysteine are sulfur amino acids that play important roles in many biochemical reactions. Methionine, an essential amino acid, can be irreversibly converted into cysteine in a series of reactions. Methionine is first converted into AdoMet (*S*-adenosylmethionine), which serves as a methyl donor in various transmethylation reactions. A product of these transmethylations, *S*-adenosylhomocysteine, is further converted into homocysteine, which is a key intermediate in the metabolism of sulfur amino acids. In animal tissues, homocysteine is universally remethylated to methionine by methionine synthase using methyltetrahydrofolate as the methyl donor. In addition, a number of tissues can convert homocysteine into cystathionine and further to cysteine via the transsulfuration pathway through two PLP (pyridoxal 5*-phosphate)-dependent enzymes, CBS (cystathionine β-synthase) and CGL (cystathionine γ-lyase) [1].

CBS is a cytosolic enzyme that catalyses the formation of cystathionine with the release of water or hydrogen sulfide, depending on whether homocysteine is condensed with serine or cysteine. The human and rodent CBSs that have been characterized are tetrameric enzymes and each of their ~63 kDa polypeptide chains contains three different domains. The N-terminal domain binds haem, the presence of which has been suggested to increase CBS activity during the oxidation of the intracellular environment [1a,2]. Other studies suggest that haem may play a structural role that is necessary for the correct folding of the CBS protein [3,4]. The middle portion of the polypeptide chain forms the catalytic domain and is well conserved among the fold-type II PLP-dependent proteins [5]. The C-terminal domain possesses two defined CBS domains, a hydrophobic domain, CBS1, and a less conserved domain, CBS2, that are together referred to as the Bateman domain. Together, these two CBS domains bind AdoMet, an allosteric activator of mammalian CBS [6]. The C-terminal domain of mammalian CBS is also thought to be responsible for multimerization of the enzyme into homotetramers and higher oligomeric forms [6,7]. The C-terminal autoinhibitory domain of mammalian CBS can be removed by *in vitro* or *in vivo* proteolytic processing, yielding a ~45 kDa truncated form (45CBS) that forms dimers and is more active than the full-length enzyme [6,8,9].

The canonical domain architecture of mammalian CBSs is not conserved across phyla. The CBS enzymes of *Saccharomyces cerevisiae, Trypanosoma cruzi* and *Drosophila melanogaster* have been experimentally characterized; the N-terminal haem-binding domain is absent in yeast and protozoan CBS, in contrast with its presence in *Drosophila* [10–12], whereas the catalytic domain is conserved in the CBS enzymes of all three of these species. The C-terminal portion exhibits the highest degree of variability. The yeast and *Drosophila* CBS proteins contain the Bateman domain, but lack a response to AdoMet. Interestingly, although the C-terminal portion of the yeast CBS inhibits the activity of the enzyme and supports the formation of tetramers and octamers [13], *Drosophila* CBS forms only dimers [12]. In contrast, the protozoan CBS does not contain the Bateman domain and is not activated by AdoMet. Although its C-terminus is shortened, the protozoan CBS is still able to form tetramers [11]. The phylogenetic variability in the domain architecture of CBSs suggests that the activity of these enzymes is regulated differently in evolutionarily distant organisms.

In the present study, we characterized the structural and functional properties of the CBS in *Caenorhabditis elegans*, a

Abbreviations used: AdoMet, *S*-adenosylmethionine; BN, blue native; BS^3, bis(sulfosuccinimidyl) suberate; CBS, cystathionine β-synthase; CGL, cystathionine γ-lyase; DTT, dithiothreitol; EST, expressed sequence tag; GFP, green fluorescent protein; LC–MS/MS, liquid chromatography–tandem MS; PLP, pyridoxal 5*-phosphate; RNAi, RNA interference; RT, reverse transcription; SEC, size-exclusion chromatography; UTR, untranslated region; WT, wild-type.

[1] To whom correspondence should be addressed (email Viktor.Kozich@LF1.cuni.cz).

well-established model organism used to study human diseases. We first identified a transcriptionally active gene encoding CBS in *C. elegans*, we then determined its pattern of expression and characterized the enzymatic and structural properties of the encoded protein. Finally, we determined the phenotypic effects of *cbs-1* inhibition using RNA-mediated interference. These data describe novel structural features that are unique among CBS enzymes and provide the first insight into the metabolism of sulfur amino acids and hydrogen sulfide in *C. elegans*.

EXPERIMENTAL

C. elegans strains

The WT (wild-type) *C. elegans* Bristol strain N2 was obtained from the *C. elegans* Stock Center (University of Minnesota, Minneapolis, MN, U.S.A.), and the RB839 strain carrying the *F54A3.4* (*ok666*) allele was provided by the *C. elegans* Gene Knockout Consortium (Oklahoma Medical Research Foundation, Oklahoma City, OK, U.S.A.). Worm cultures were maintained as described previously [14].

Bioinformatics

BLASTp searches were performed by online BLAST software using the *C. elegans* protein database (release WS215). Protein domain modelling was performed by Swiss-model (automatic modelling mode) using the crystal structure of human 45CBS (PDB code 1JBQ, chain A) as a template [15]. PDB structures were subsequently evaluated in the Prosa program [16] and visualized in Swiss-PDBViewer 4.0.4 [17]. Phylogenetic trees were constructed in the online portal system Mobyle [18]. Multiple alignments of amino acid sequences were performed using ClustalW2 online software with default parameters [19]. Conserved regions were also separated for further analysis by ClustalW2. For phylogenetic analysis, alignment was bootstrapped 100 times and analysed by the maximal likelihood method using the PHYML 3.0 program [20]. Bootstrap output trees were analysed by the PHYLIP 3.67 CONSENSE program; the final tree shape was visualized in the Dendroscope program [21].

PCR amplification and DNA sequencing

Nematode cDNA was prepared by RT (reverse transcription) using isolated total RNA from mixed stages of N2 worms and a RT kit with an oligo(dT) primer (Promega). Open reading frames of *ZC373.1* and *F54A3.4* were amplified by PCR using either cDNA prepared by RT–PCR or a *C. elegans* cDNA library (Invitrogen) as the template (a list of the primers is given in Supplementary Table S1 at http://www.BiochemJ.org/bj/443/bj4430535add.htm). PCR products were cloned into the pCR4-TOPO vector (Invitrogen), and the authenticity of the DNA sequence was verified by dideoxy sequencing using an ABI PRISM 3100-Avant sequencer (Applied Biosystems).

GFP (green fluorescent protein) reporter assay

To determine the expression pattern of *cbs-1*, we generated a translational fusion vector using the PCR fusion technique described previously [22]. The 1.8 kb of 5′ upstream sequence and the entire coding region of *ZC373.1* were amplified by PCR using primers A and B (Supplementary Table S1), and genomic *C. elegans* DNA as a template. The vector pPD95.75 was used as a template for amplification of the GFP-coding sequence using primers C and D (Supplementary Table S1). The two PCR products were mixed and used as a template for PCR fusion using nested primers E and F (Supplementary Table S1). The 6.8-kb PCR product was injected into *C. elegans* hermaphrodite gonads together with the plasmid pRF4 as a phenotypic marker for injection. Transgenic animals were separated, and the F2 progeny were screened for the GFP signal. An Olympus BX60 microscope and a Nikon Eclipse E800 with C1 confocal module and 488 nm laser and differential interference contrast optics were used for specimen examination.

Bacterial expression and protein purification

Initially, recombinant CBS-1 was expressed as a fusion protein with an N-terminal GST tag and further purified by affinity chromatography to 75 % purity (see Supplementary Figure S4, lane 6) according to a previously described procedure for human CBS [23]. The contaminating polypeptide with the highest abundance, a 40-kDa fragment that represented approximately 20 % of the total protein, was identified as the N-terminal portion of CBS-1 (residues 1–375) by peptide mass fingerprinting using MS detection (results not shown). This N-terminal fragment was observed with similar abundance even when the purification procedure was modified to limit proteolytic cleavage of the recombinant protein (the modification involved performing affinity chromatography at 4 °C and increasing the concentration of protease inhibitors in the bacterial crude extract). To overcome this obstacle that was not previously reported for other CBS orthologues, we constructed a new vector that produced double-tagged CBS-1 with a cleavable N-terminal GST tag and a C-terminal His tag. The open reading frame of the *ZC373.1* gene encoding CBS-1 was amplified by PCR using a *C. elegans* cDNA library as the template. PCR was performed with Taq polymerase using primers P and R (Supplementary Table S1). The 2.1-kb DNA fragment obtained by digestion of the PCR product with BamHI and XhoI was cloned into the BamHI- and XhoI-digested pGEX-6p-1 vector. Express Competent *Escherichia coli* cells (New England Biolabs) were transformed with the plasmid that encodes double-tagged CBS-1 (GST–CBS–1–His_6) and cultured in the presence of 100 μM IPTG (isopropyl β-D-thiogalactopyranoside) at 18 °C for 24 h. The GST–CBS-1 fusion protein was purified according to the purification protocol for human CBS described previously [24] with the following modifications: after cleavage by the PreScission protease (GE Healthcare), recombinant CBS-1 was loaded on to a Ni-Sepharose column that had been equilibrated with IMAC buffer [20 mM phosphate (pH 7.5), containing 0.5 M NaCl, 20 mM imidazole and 1 mM DTT (dithiothreitol)]. The column was washed with IMAC buffer containing 50 mM imidazole. CBS-1 was then eluted with IMAC buffer containing 75 mM imidazole. The protein enrichment procedure yielded approximately 1 mg of CBS-1 per litre of bacterial culture. The purity of isolated CBS-1 was analysed by SDS/PAGE [pre-cast 3–8 % gradient gel (Invitrogen)] with Coomassie Brilliant Blue staining. The protein concentration was determined using Bradford reagent (Sigma–Aldrich) with BSA as the standard. The absorption spectrum of CBS-1 was recorded using a UV–visible spectrophotometer (Shimadzu UV-2550) at room temperature (25 °C).

SEC (size-exclusion chromatography)

SEC was performed on an HPLC platform (Shimadzu LC-10A system). Recombinant purified CBS-1 was loaded on to a Bio-Sil SEC HPLC column (catalogue number 125-0060, Bio-Rad

Laboratories) that had been previously equilibrated with buffer containing 50 mM Tris/HCl (pH 8.0), 1 mM DTT and 100 mM NaCl. The analysis was performed at a flow rate of 1.0 ml/min at 25 °C; the elution profile was obtained by measurement of the absorbance at 280 nm. Calibration was performed using ferritin, aldolase, conalbumin (GE Healthcare), BSA (Thermo Fisher Scientific) and human 45CBS produced in *E. coli* and purified as described previously [24].

Native PAGE, BN (blue native)-PAGE and chemical cross-linking

Native electrophoresis was performed on 8 % polyacrylamide gels using the Laemmli buffer system without SDS [25]. Per lane, 5 μg of CBS-1 and of the standards (BSA and human 45CBS) were loaded. BN electrophoresis was performed as described previously [26] with the High Molecular Weight Calibration kit for electrophoresis (GE Healthcare) and rabbit aldolase as the protein marker. Chemical cross-linking was performed using three different concentrations of BS^3 [bis(sulfosuccinimidyl) suberate]; the molar ratios of CBS-1 (0.5 mg/ml) to the cross-linker were 1:10, 1:50 and 1:100. Cross-linked proteins were analysed using precast 3–8 % gradient polyacrylamide gels. As a positive control for efficient cross-linking, we used dimeric human 45CBS reacted with BS^3 at a protein/cross-linker molar ratio of 1:10. All of the proteins analysed by electrophoretic techniques were stained with EZ Blue Gel reagent (Sigma–Aldrich).

Pulse proteolysis

Pulse proteolysis of CBS-1 in a urea gradient was performed with thermolysin as described previously for human CBS [27].

Fluorescence-based thermal-shift assay

Protein samples (0.5 mg/ml) were dissolved in 20 mM Tris/HCl (pH 8.0), and 5×Sypro Orange dye (Bio-Rad Laboratories). Using the real-time PCR Detection System CFX96 Touch (Bio-Rad Laboratories), the proteins were incubated in a thermal gradient from 25 °C to 70 °C at increments of 0.5 °C and with 1-min-hold intervals. The degree of protein unfolding was monitored by a FRET (fluorescence resonance energy transfer) channel that captured the spectral properties of Sypro Orange unfolded protein complexes (excitation wavelength ≈ 470 nm and emission wavelength ≈ 570 nm). The data were analysed by CFX Manager software, and the melting temperatures were determined using the first derivative spectra.

CD and fluorescence spectroscopy

The CD spectra of CBS-1 protein variants [0.5 mg/ml in 50 mM phosphate buffer (pH 7.5)] were recorded using a Jasco J-810 chiroptic spectrometer. The intrinsic fluorescence of CBS proteins in 50 mM Tris/HCl (pH 8.0), was measured in the same buffer using a PerkinElmer LS55 fluorescence spectrometer. The excitation wavelength for tryptophan was 298 nm (slit width of 5 nm) with an emission signal scanned from 300 to 700 nm (slit width of 5 nm).

Determination of substrate specificity

All enzyme assays were performed at 25 °C with an incubation time of 10 min to ensure a linear increase in cystathionine or cysteine production. The reaction mixtures (50 μl) contained 1 μg/ml purified recombinant CBS-1, 10 mM tested substrates in the combinations shown in the Results section, 1 mM PLP, 1 mM DTT, 1 mg/ml BSA and 150 mM Tris/HCl (pH 7.0). The reactions were stopped by the addition of 25 μl of 1 M trichloracetic acid, and the reaction products were determined by HPLC [28] or LC–MS/MS (liquid chromatography–tandem MS) analysis [29] with the modifications described below.

Temperature and pH optima and kinetic analysis

We measured cystathionine production using LC–MS/MS analysis [29] with the following modifications: assays were performed in 100 mM Bis/Tris buffer with 2 μg/ml purified recombinant CBS-1 and unlabelled serine as the substrate. The temperature optimum for CBS-1 activity was determined in 5 °C temperature intervals from 5 °C to 80 °C at pH 8.0, and the pH optimum of CBS-1 was determined at 25 °C in 0.5 pH unit intervals using 100 mM Bis/Tris buffer at pH 6–10. Kinetic analyses at different concentrations of serine or homocysteine were performed at 25 °C and pH 8.0, and the data were evaluated by non-linear data fitting using software Origin 8 (OriginLab). All measurements were repeated four times and the results are shown as means ± S.D.

Site-directed mutagenesis and preparation of CBS-1 protein variants

We prepared and analysed a series of mutant CBS-1 enzymes that included two missense variants of full-length CBS-1 (E62K and K421A) and six truncated CBS-1 variants (CBS-1b, Δ1–372, Δ1–322, Δ1–299, b/360 and b/375) (Figure 4A). All CBS-1 variants were cloned into the pGEX vector, which produces GST-tagged proteins. The sequences of primers used for cloning and site-directed mutagenesis are shown in Supplementary Table S1. Proteins were expressed and purified according to the procedure developed for CBS-1. The yields of purified mutant proteins were slightly lower, typically approximately 0.5 mg per litre of bacterial culture. The mutant proteins were analysed by UV–visible spectroscopy, CD and fluorescence spectroscopy and by BN-PAGE as described above for CBS-1. The catalytic activities for the reaction of serine with homocysteine were assessed in 100 mM Tris/HCl (pH 8.5) at 25 °C.

RNA-mediated interference

The *cbs-1*-specific sequence (~ 350 bp in length) was prepared by PCR amplification of a *C. elegans* cDNA library primers G and H (Supplementary Table S1) and cloned into the pCR4-TOPO vector. Single-stranded RNAs were prepared from linearized DNA by *in vitro* transcription using T3 DNA-dependent RNA polymerase (construct DNA digested by NotI) and T7 DNA-dependent RNA polymerase (construct DNA digested by SalI). The sense and antisense single-stranded RNAs were mixed and incubated at 68 °C for 10 min, followed by incubation at 37 °C for 30 min. The double-stranded RNA was further purified by phenol/chloroform extraction and precipitated by ethanol; the RNA pellet was diluted in water to an approximate concentration of 2 μg of RNA/μl. The double-stranded RNA was injected into the gonads of young adult hermaphrodite worms as described previously [30]. The embryos of microinjected animals were synchronized in 9–12 h intervals. Nematodes were grown at 16 °C on nematode growth medium plates and fed with *E. coli* strain OP50. After RNAi (RNA interference), the nematodes were seeded in 1× PBS buffer on 2 % agarose and screened by their phenotype.

Determination of CBS-1 antigen levels and measurement of enzymatic activity in *C. elegans* extracts

Worms were grown at 16 °C as described above and collected 7 days after embryo microinjection as a mixed population of all larval stages. Worm lysates were prepared by sonication of worm pellets resuspended in 1 vol. of 100 mM PBS containing protease

inhibitor cocktails for prokaryotic (P8465, Sigma–Aldrich) and eukaryotic (P8340, Sigma–Aldrich) cells. Crude extracts were centrifuged for 1 h at 4 °C and 20000 ***g*** and the supernatants were used for the determination of CBS-1 levels and CBS activity. Western blotting was used to examine CBS-1 antigen levels after RNAi. The samples were submitted to SDS/PAGE (pre-cast 3–8 % gradient gel), and protein immunodetection was performed by Western blot analysis using custom-made rabbit polyclonal anti-CBS-1 antibody prepared against purified recombinant CBS-1 (Exbio Praha). Actin, which was detected using a rabbit anti-actin antibody (Abcam), was used for the normalization of protein loading. The signal levels of CBS-1 and actin were determined by chemiluminescence (Pierce) by employing the ChemiGenius station and Gene Tools software for semi-quantification [31]. The enzyme assay was performed according to a previously described protocol [29] with the modification that the reaction mixture was incubated at 16 °C for 30 min.

Measurement of metabolites in *C. elegans* extracts

Worm lysates were prepared by sonication of worm pellets that had been resuspended in 1 vol. of 100 mM PBS without protease inhibitors (Cole-Parmer GE130 Ultrasonic processor, amplitude 20 for 2 min with 1 s on/off pulses). The crude extracts were centrifuged at 20000 ***g*** for 1 h at 4 °C, and the supernatants were used for HPLC aminothiol determination as described previously [28]. The cystathionine concentration was determined by LC–MS/MS using the EZ:faast kit for amino acid analysis (Phenomenex) [29]. The concentrations of all metabolites measured were normalized to the amount of protein present in the sample.

RESULTS

CBS in *C. elegans* is encoded by *ZC373.1*

We used a BLASTp search as an *in silico* approach to identify genes that encode a CBS in *C. elegans*. Using the query sequences of three enzymes of the CBS family (human CBS, trypanosomal CBS and bacterial cysteine synthases), we identified ten genes with predicted amino acid sequences that are homologous with the catalytic domains of the known CBSs; these genes are annotated in WormBase (http://www.wormbase.org/) as 'CBS and related proteins'. Alignment of the predicted amino acid sequences of the *C. elegans* genes *ZC373.1* and *F54A3.4* revealed the highest homology with human CBS (UniProt entry P35520). These predicted proteins exhibited 54 % sequence identity with the human protein, whereas the other eight predicted proteins showed lower homology, with 21–44 % sequence identity (Supplementary Table S2 at http://www.BiochemJ.org/bj/443/bj4430535add.htm). The BLASTp searches using all ten nematode CBS homologues as the query sequences against the UniProt database, together with phylogenetic analysis, indicated that only ZC373.1 and F54A3.4 are homologous with CBS, whereas the remaining eight amino acid sequences are homologous with other proteins within the family of fold-type II PLP-dependent enzymes (Supplementary Figure S1 at http://www.BiochemJ.org/bj/443/bj4430535add.htm).

An annotation in the WormBase database shows that the *ZC373.1* gene is trans-spliced to SL1 and contains ten exons, including 23 bp of the 5′-UTR (untranslated region) and 149 bp of the 3′-UTR followed by a polyadenylation sequence. The *F54A3.4* gene is predicted to contain either eight exons without any 5′- or 3′-UTRs (http://www.wormbase.org/) or only seven exons terminated by a 77 bp 3′-UTR sequence (http://www.ncbi.nlm.nih.gov/IEB/Research/Acembly/). To determine whether the *ZC373.1* and *F54A3.4* genes are transcribed and spliced into the predicted full-length mRNAs, we analysed their coding regions by RT–PCR and by sequencing of PCR products. We found two differently spliced variants of the *ZC373.1*; one sequence is identical with the WormBase annotation (*cbs-1*), and the other is a new *ZC373.1* splice variant (*cbs-1b*) containing a 5-bp shortening of exon 7 in its 5′-terminus that leads to a frame-shift with a premature stop codon at amino acid residue 377 (Figure 1A and Supplementary Figure S2 at http://www.BiochemJ.org/bj/443/bj4430535add.htm). In contrast, we were unable to amplify either of the two hypothetical full-length *F54A3.4* mRNAs using several PCR conditions, various primers and various cDNA templates.

Because we did not succeed in detecting the *F54A3.4* mRNA by RT–PCR, we used additional approaches to examine the possible role of this gene in *C. elegans*. *In silico* analysis of the GenBank® database revealed three ESTs (expressed sequence tags) of *F54A3.4*: CK587466.1, CB389123.1 and FN902238.1; however, only FN902238.1 has been mapped to the sense strand of the *F54A3.4* region (http://www.ncbi.nlm.nih.gov/nucleotide/). Furthermore, the proteomic database PeptideAtlas did not contain any peptide matches to the hypothetical protein F54A3.4 (http://www.peptideatlas.org/) [32]. Moreover, expression analysis using translational fusion proteins F54A3.4–GFP and ZC373.1–GFP (cbs-1–GFP) (see below) showed that the GFP signals reflecting the expression pattern of the appropriate genes were observed only in worms carrying ZC373.1–GFP, in contrast with the expression patterns observed in several worms carrying F54A3.4–GFP. Finally, *F54A3.4* does not appear to have functional significance in *C. elegans* because the mutant strain RB839, which carries a deletion of *F54A3.4*, showed CBS activity and homocysteine concentrations indistinguishable from those of the WT strain (results not shown), and did not exhibit abnormal behavioural or a developmental phenotype (results not shown).

On the basis of the findings listed above, *F54A3.4* appears to be a pseudogene and was not further examined in the present study. All of the data above strongly indicate that the *C. elegans* genome contains only one expressed orthologue of the human CBS gene, i.e. *ZC373.1*. In accordance with the recommended nomenclature, this gene was named *cbs-1*.

CBS-1 is a cytoplasmic enzyme that is expressed in the hypodermis and intestine, and in muscle cells

To determine the expression pattern and subcellular localization of *cbs-1*, we constructed the translational vector cbs-1–GFP, which contains the promoter and the entire CBS-1 sequence tagged at the C-terminus with GFP (Figure 1A). In worms expressing cbs-1–GFP, the GFP signal was observed in the hypodermis, intestine, body-wall muscle cells and pharyngeal muscles pm3, pm4, pm5, pm6, pm7 and pm8 in all larval stages as well as in adults (Figure 2). Our data using a translational reporter showed a similar expression pattern, as did previous transcriptional screens, and a novel expression of *cbs-1* in pharyngeal muscles. We did not observe a GFP signal in embryos, although previous transcriptional screens and peptide mapping studies have reported expression of *cbs-1* in this developmental stage [32,33]. The observed GFP signal was distributed diffusely within cells and spared the nucleus, suggesting that CBS-1 is localized in the cytoplasm. These data provide the first reported insight into the tissue and subcellular localization of nematode CBS-1 at the protein level and indicate which nematode tissues can metabolize homocysteine to cystathionine and/or cysteine to hydrogen sulfide.

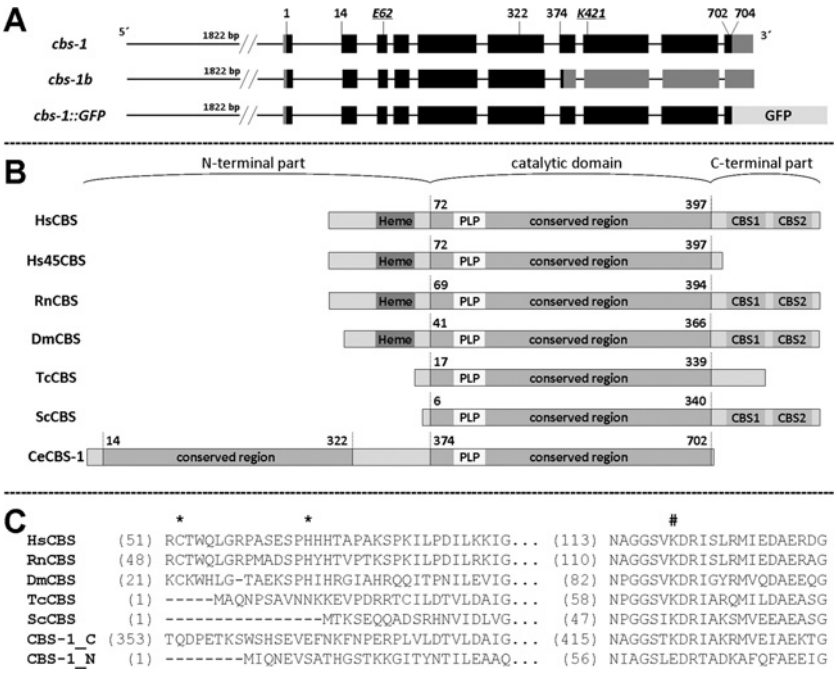

Figure 1 Organization of the *cbs-1* gene and domain architecture of CBS in various organisms

(**A**) Gene organization. The top diagram shows the organization of gene *ZC373.1* (*cbs-1*) encoding CBS-1. The numbers indicate the codon position encoding the appropriate amino acid. Exons are indicated as black boxes, and the 5′- and 3′-UTR sequences are indicated as grey boxes. The middle diagram shows the novel splice *ZC373.1* variant *cbs-1b*. The bottom diagram shows the translational fusion construct used in the GFP reporter assay. The length of the entire promoter used in the cbs-1–GFP construct is indicated by the number of base pairs of the 5′-upstream sequence. (**B**) Domain organization of various CBSs. The published structures of different CBSs were analysed for the presence of a haem-binding site (marked Heme), conserved catalytic regions with a PLP-binding site (marked PLP) and Bateman domain composed of two CBS domains (CBS1 and CBS2). The primary structures are aligned by the PLP-binding lysine residue; the numbers indicate the first and the last amino acid residues of conserved domains in the protein sequence. The aligned proteins are HsCBS (*Homo sapiens* CBS, UniProt entry P35520), Hs45CBS (truncated human CBS with 1–413 residues), RnCBS (*Rattus norvegicus* CBS, UniProt entry P32232), DmCBS (*D. melanogaster* CBS, UniProt entry Q9VRD9), TcCBS (*T. cruzi* CBS, UniProt entry Q9BH24), ScCBS (*S. cerevisiae* CBS, UniProt entry P32582) and CBS-1 (*C. elegans* CBS, UniProt entry Q23264). (**C**) Amino acid alignment of haem- and PLP-binding sites in various CBSs with separated N- and C-terminal conserved regions of CBS-1. The N-terminal region of CBS-1 does not contain the lysine residue that binds PLP. The cysteine and histidine residues that bind haem are indicated by asterisks, and the PLP-binding lysine residues are indicated by #.

CBS-1 is a haem-independent protein that lacks activation by AdoMet

To experimentally characterize the structural and enzymatic properties of CBS-1, *cbs*-1 cDNA was expressed in *E. coli*. Recombinant CBS-1 (704 residues of native CBS-1 with five additional amino acids at the N-terminus, six additional histidine residues at the C-terminus and a size of ~78 kDa) was purified to greater than 95% purity (Supplementary Figure S4 at http://www.BiochemJ.org/bj/443/bj4430535add.htm). The UV–visible absorption spectrophotometry of the purified recombinant CBS-1 showed a peak at 412 nm, confirming the presence of covalently bound PLP that forms an internal aldimine, but it did not reveal a Soret band associated with a haem moiety (Figure 4F). This analysis confirmed that, in contrast with other characterized metazoan CBS enzymes, the nematode enzyme is a haem-independent CBS.

We next tested four reactions that have been described for previously characterized CBSs: (i) cystathionine-synthesizing activity that produces cystathionine and water from homocysteine and serine; (ii) formation of cystathionine and hydrogen sulfide from homocysteine and cysteine; (iii) cysteine synthase activity that produces cysteine from *O*-acetylserine and hydrogen sulfide; and (iv) serine sulfhydrylase activity in which cysteine is synthesized from serine and hydrogen sulfide. CBS-1 exhibited high enzymatic activity for synthesis of cystathionine from homocysteine utilizing either serine or cysteine and considerably lower cysteine synthase and serine sulfhydrase activities for synthesis of cysteine. The specific activities of CBS for the production of cystathionine from serine and cysteine were $\sim 1500\ \mu mol \cdot h^{-1} \cdot mg^{-1}$ and $\sim 300\ \mu mol \cdot h^{-1} \cdot mg^{-1}$ respectively, and its specific cysteine synthase and serine sulfhydrase activities were $\sim 5\ \mu mol \cdot h^{-1} \cdot mg^{-1}$ and $\sim 30\ \mu mol \cdot h^{-1} \cdot mg^{-1}$ respectively. None of these activities were stimulated by 1 mM AdoMet (results not shown), which is consistent with the absence of a Bateman domain in CBS-1 (see below). These data show that the nematode CBS-1 enzyme exhibits typical CBS activity and that it is not activated by AdoMet.

CBS-1 has a unique structural arrangement

Alignment of the predicted amino acid sequence of CBS-1 with the sequences of previously characterized human, rat, *Drosophila*, trypanosome and yeast CBS enzymes revealed that the *C. elegans* enzyme possesses unique and novel domain architecture. In contrast with other CBSs, *C. elegans* CBS-1 lacks both the haem-binding N-terminus and the entire C-terminus found in other species (Figures 1B and 1C). Moreover, amino acid alignment together with protein modelling revealed that a single polypeptide chain of CBS-1 contains a unique tandem arrangement of two conserved CBS cores that belong to a family of fold-type II PLP-dependent proteins (Figure 1B and 3). Phylogenetic analysis of these two CBS-1 modules revealed that, in contrast with the C-terminal module, the N-terminal module has a lower homology with other CBS enzymes and does not belong to any of the fold-type II PLP-dependent protein families tested (Supplementary Figure S3 at http://www.BiochemJ.org/bj/443/bj4430535add.htm).

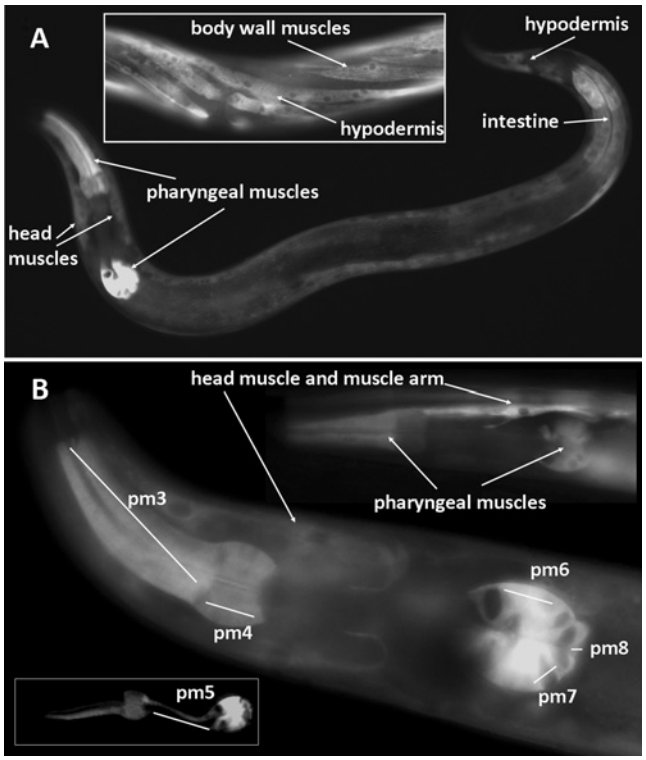

Figure 2 Expression pattern of *cbs-1* in worms

The images show transgenic worms that carry the translational fusion vector cbs-1–GFP. (**A**) L4 larval stage showing the distribution of the GFP signal in the pharyngeal muscles, intestine, hypodermis and muscle cells. The middle part of the adult body (inset) shows the GFP signal in the body wall muscles and hypodermis. (**B**) Head of the worm showing GFP signal in pharyngeal muscles and a head muscle cell with its muscle arm; the GFP signal is distributed in the pharyngeal muscles pm3, pm4, pm6, pm7 and pm8. Some worms also exhibited a GFP signal in pm5 (inset).

Furthermore, the critical PLP-binding lysine residue in the N-terminal module is replaced by a glutamic acid residue (Figures 1C and 3). Analysis of the PLP-binding site using homology modelling with the structure of 45CBS as the template revealed that the fully conserved glycine residue (Gly^{256} in human 45CBS) in the N-terminal module is replaced by a bulky asparagine residue (Asn^{197}) that may sterically affect PLP binding (Figure 3). Thus the *in silico* data strongly suggest that the N-terminal module of nematode CBS-1 cannot bind the PLP essential for the catalytic activity of the enzyme.

The catalytic activity of CBS-1 is mediated only by the C-terminal module

To confirm the hypothesis that the catalytic function of CBS-1 is mediated only by its C-terminal module, we generated individual CBS-1 modules in *E. coli*. While the CBS-1b variant, which lacks the C-terminal module of CBS-1, was highly soluble after expression in *E. coli*, all of the cloned CBS-1 variants without the N-terminal module showed substantially decreased solubility (Figure 4B) that prevented successful purification of proteins containing only the C-terminal module. However, we purified and characterized the CBS-1b and used UV–visible and fluorescence spectrometry to determine that it does not bind PLP; we also found that CBS-1b had virtually undetectable catalytic activity (Figures 4D, 4F and 4G and Table 1). These observations demonstrate that the PLP-binding site essential for catalytic activity is not located in the N-terminal module of the CBS-1 protein. Although CD spectrometry showed that the CBS-1b has a helical secondary structure similar to that of the WT CBS-1 protein (Figure 4E), BN-PAGE revealed that purified CBS-1b precipitates and may form higher-order oligomers (Figure 4C). These data indicate that the presence of both CBS-1 modules in one subunit is necessary for the maintenance of the global structural stability of CBS-1 and/or for proper folding of the recombinant protein.

Because analysis of the isolated N-terminal module indicated possible disruption of its native structure, we also generated and purified the CBS-1 mutants K421A, which abolishes a canonical PLP-binding site in the C-terminal module, and E62K, which creates a putative PLP-binding site in the N-terminal module. We observed altered fluorescence-based tryptophan spectra of the mutant proteins; their relative fluorescence showed different quenching of the tryptophan emission, and the existence of a wavelength maximum shift from ~340 to ~350 nm indicates higher accessibility of the tryptophan residues to the polar solvent in the K421A mutant (Figure 4G and Table 1). In contrast, both mutants retained oligomeric status identical with the WT as determined by BN-PAGE (Figure 4C), and CD measurements showed that the protein's secondary structure is not affected by either the K421A or E62K mutation (Figure 4E). The catalytic activity, PLP saturation and fluorescent properties of the E62K mutant were similar to those of WT (Figures 4D, 4F and 4G), supporting the idea that the structural properties of the N-terminal module do not permit PLP binding even if the canonical lysine residue is present. In contrast, the K421A mutant binds significantly less of the PLP cofactor, as determined by UV–visible absorption spectroscopy. The mutant enzyme's residual affinity for PLP probably results from the formation of an external aldimine; this affinity is manifested in its UV–visible spectrum by the presence of two bands with maxima at 403 and 418 nm and by the lack of the sharp maximum at 412 nm that is typical for internal aldimines (Figure 4F). The formation of an external aldimine in K421A was confirmed by fluorescence spectroscopy and, when excited at 298 nm, the emission spectrum of the mutant protein revealed a significantly higher extent of delayed fluorescence of Schiff bases for K421A in comparison with WT, E62K and CBS-1b (Figure 4G). Enhanced delayed fluorescence due to formation of external aldimines in the active site of the mutant enzyme has also been reported for the bacterial *O*-acetylsulfhydrylase mutant K42A [34]. Taken together, these experiments provide additional evidence that the catalytic activity of *C. elegans* CBS-1 is mediated only by the C-terminal module and that its N-terminal module cannot bind PLP cofactor either as an internal or as an external aldimine.

Analysis of the quaternary structure of nematode CBS-1 suggests a monomeric status of CBS-1

We analysed the quaternary structure of recombinant nematode CBS-1 to determine whether CBS-1 exists as a monomer with a structural arrangement similar to human 45CBS (the C-terminally truncated human CBS that lacks a Bateman domain and forms dimers of 90 kDa [15]), or whether CBS-1 forms dimers or higher-order oligomers. We first performed SEC using the standard proteins ferritin (440 kDa), aldolase (158 kDa), conalbumin (75 kDa) and BSA (66 kDa). To control for possible differences in the Stokes radii of the standard proteins and the CBS-related proteins that may influence their retention on the column, we analysed human 45CBS in parallel. Nematode CBS-1 exhibited a tailing peak with a retention time of 5.776 min (Figure 5A); on the basis of the calibration curve, the apparent native molecular mass of the protein was determined to be ~170 kDa. However, SEC of human 45CBS indicated a native molecular mass of

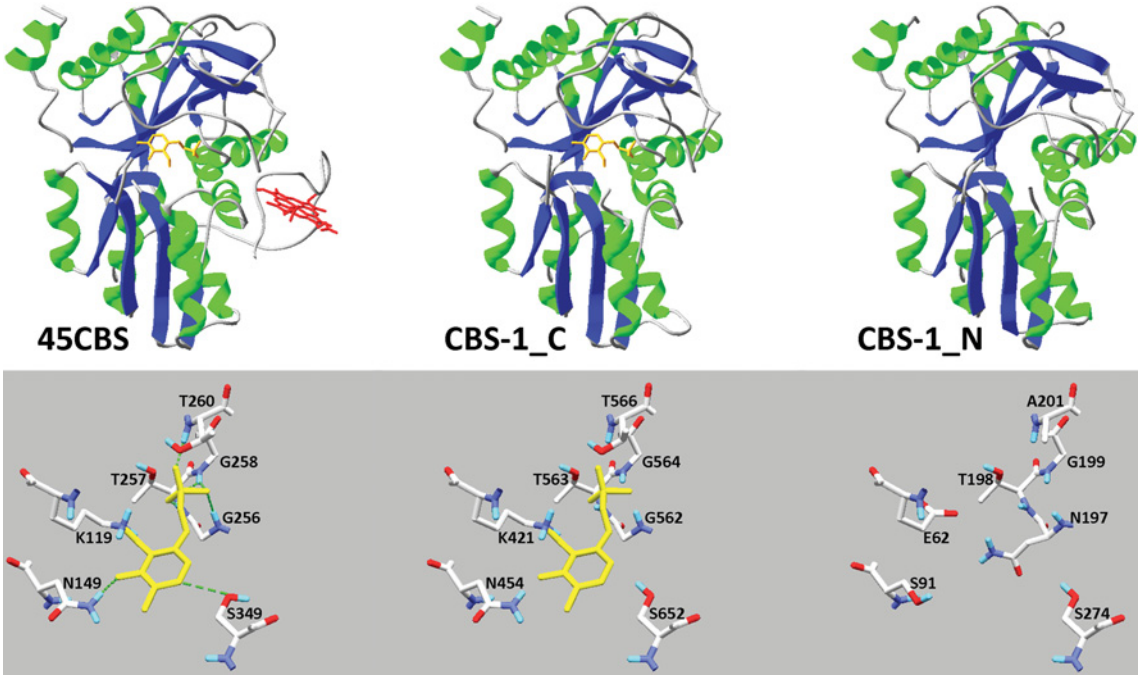

Figure 3 Computationally modelled CBS-1 domains

The images show the fold and PLP-binding site of human 45CBS, C-terminal module of CBS-1 (CBS-1_C) and N-terminal module of CBS-1 (CBS-1_N). The crystal structure of the human enzyme shows hydrogen bonds between amino acid residues and PLP, as indicated by broken green lines. Computational modelling of the individual CBS-1 modules revealed that both modules belong to the family of fold-type II PLP-dependent proteins and that the N-terminal module cannot bind PLP due to the absence of lysine and glycine residues in the consensus PLP-binding pocket.

approximately 150 kDa, suggesting that calibration with standard proteins may result in overestimation of the molecular mass of CBS proteins. According to the molecular mass markers used, SEC yielded ambiguous results compatible with both a monomeric and dimeric structure of CBS-1.

We next used additional techniques including native electrophoresis, BN electrophoresis and chemical cross-linking followed by SDS/PAGE to determine the most likely quaternary structure of CBS-1. These three techniques congruently showed that the 78 kDa nematode CBS-1 exists predominantly as a monomer. The evidence, which is shown in Figures 5(B)–5(D), is as follows: (i) in native PAGE, nematode CBS-1 migrates similarly to the 90 kDa marker of dimeric human 45CBS and between fractions containing monomeric and dimeric BSA respectively (66 kDa and 132 kDa); (ii) on BN electrophoresis, CBS-1 migrates between molecular mass markers of 66 and 140 kDa; and (ii) chemical cross-linking of CBS-1 did not result in changes in protein migration, suggesting modification of amino acid side chains within a single polypeptide chain, whereas human 45CBS readily formed a cross-linked dimeric product with a molecular mass of ~100 kDa. On the basis of these results, we propose that, in contrast with CBS enzymes from other species, recombinant nematode CBS-1 does not form oligomeric structures *in vitro*. Because the conserved catalytic regions of CBS-1 are homologous with each other, we hypothesize that they form an internal interface similar to that formed by subunit dimerization of human 45CBS (Figure 5E).

CBS-1 is more sensitive to denaturation and is more active than human 45CBS

We hypothesized that the above-described differences in the oligomeric assembly of nematode CBS-1 and human 45CBS might result in differences in the energetics of the two proteins. To explore this hypothesis, we used a fluorescence-based thermal-shift assay and pulse proteolysis in a urea gradient. Both approaches revealed significantly lower stability of CBS-1 compared with the human 45CBS; the melting point of CBS-1 was 10 °C lower than that of human 45CBS, and the resistance of CBS-1 to urea-induced unfolding decreased by ~2.8 M (Table 2 and Supplementary Figure S5 at http://www.BiochemJ.org/bj/443/bj4430535add.htm). These data show that the nematode CBS-1 is less energetically stable than the human 45CBS; this finding may be due to a lower energy of the interdomain interface or a higher structural flexibility of the worm CBS-1.

We considered the possibility that the observed structural and energetic differences between the nematode CBS-1 and human 45CBS result in different catalytic properties. We determined the temperature and pH optima and the kinetic parameters for the major CBS reaction, which produces cystathionine from serine and homocysteine. The CBS-1 protein exhibited the highest activity at pH 8.5 and 30 °C (Supplementary Figure S6 at http://www.BiochemJ.org/bj/443/bj4430535add.htm). These conditions are in accordance with the results of the thermal stability assay (see above). We speculate that the lower temperature optimum of CBS-1 compared with the human enzymes (37 °C) may reflect the lower body temperature of nematodes living in the soil. We also found that the affinity of CBS-1 for homocysteine is lower than that of 45CBS (Table 2); however, we observed inhibition of CBS activity at 7.5 and 10 mM homocysteine and this inhibition prevented the activity from increasing to more than ~1500 $\mu mol \cdot h^{-1} \cdot mg^{-1}$ (Supplementary Figure S6). Inhibition by high concentrations of homocysteine has been previously reported for yeast and human CBS enzymes [13,35]. Taken together, these data show that the nematode CBS-1 subunit is approximately 4-fold more active compared with the human 45CBS subunit as expressed by the turnover number (Table 2).

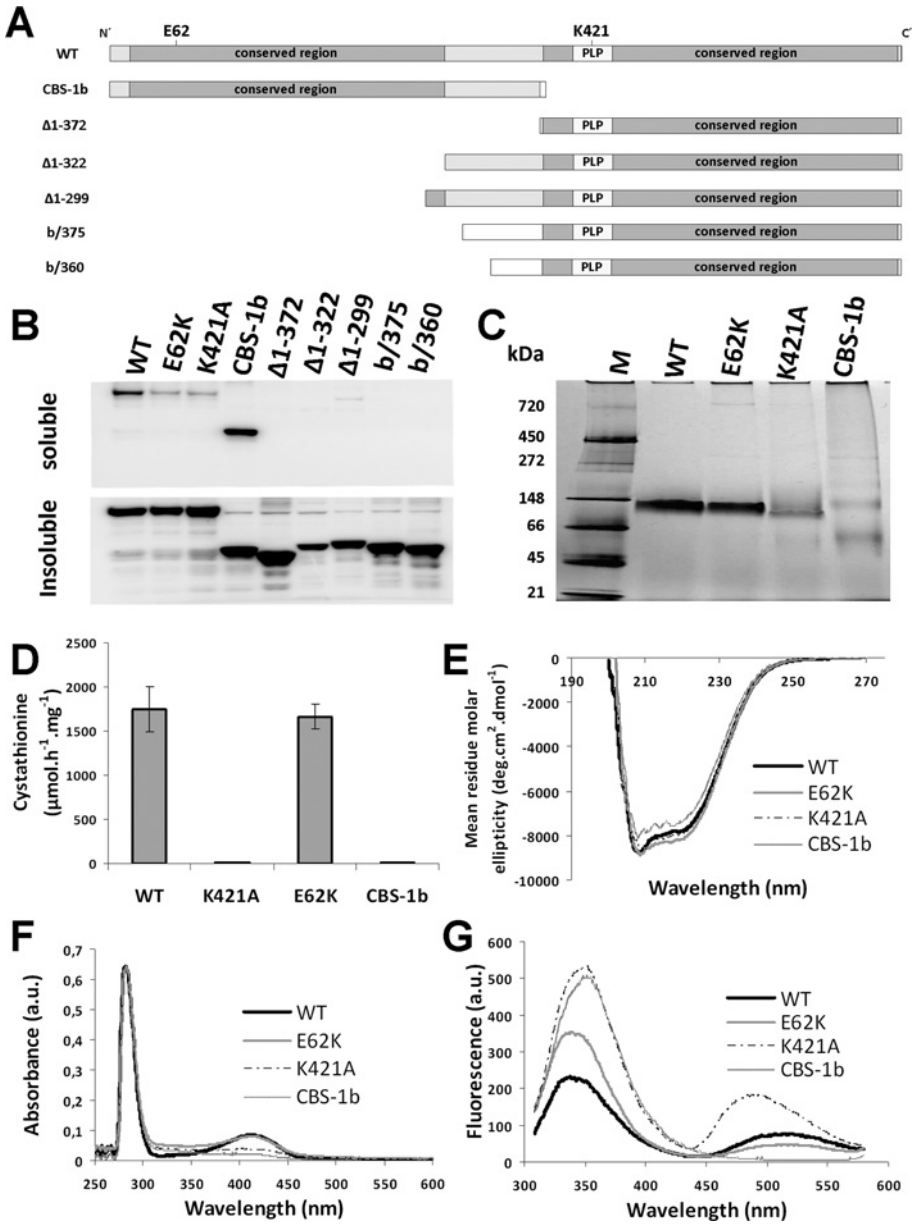

Figure 4 Structural and enzymatic analysis of recombinant CBS-1 variants

(**A**) Illustration of the CBS-1 variants expressed in *E. coli*. (**B**) Detection of CBS-1 variants in *E. coli* lysate after expression using soluble and insoluble fractions separated by centrifugation. (**C**) BN-PAGE of purified recombinant CBS-1 variants shows the monomeric status of the WT, K421A and E62K proteins. The N-terminal domain exhibits monomeric and oligomeric forms. Molecular mass markers are shown in kDa on the left-hand side. (**D**) CBS activity of the purified CBS-1 variants; K421A and CBS-1b have no CBS activity. Results are means $\pm$ S.D. (**E**) CD spectra at far-UV show a helical secondary structure for all of the purified CBS-1 variants. (**F**) The UV–visible spectrum of purified recombinant CBS-1 variants of equal concentration shows peaks in the 280 and 412 nm region, indicating light absorption by aromatic amino acids and PLP respectively. Soret peaks typical for haem are not present. (**G**) Emission spectrum after excitation of the tryptophan residues at 298 nm of purified recombinant CBS-1 variants of equal concentration.

CBS-1 mediates nematode development and maintains homocysteine homoeostasis

To explore the functional significance of *cbs-1* in *C. elegans*, we silenced the *cbs-1* gene by RNA-mediated interference and determined the phenotypic consequences of such silencing. To confirm the efficacy of *cbs-1* RNAi, we measured the amounts of CBS-1 antigen and CBS activity in worm extracts of CBS-1-inactivated and WT worms. Western blot analysis using an anti-CBS-1 antibody showed that after RNAi treatment worms exhibited a CBS-1 level that was approximately 10 % that of the control strain (Supplementary Figure S7A at http://www.BiochemJ.org/bj/443/bj4430535add.htm). Although the mean CBS activity of normal worms was 36.0 $\text{nmol} \cdot \text{h}^{-1} \cdot \text{mg}^{-1}$, *cbs-1* RNAi animals exhibited a mean activity of only 5.4 $\text{nmol} \cdot \text{h}^{-1} \cdot \text{mg}^{-1}$, approximately $\sim$15 % of the control level (Supplementary Figure S7B). The results from both Western blot analysis and CBS activity measurement consistently confirmed that the RNAi experiments efficiently reduced the amount and activity of CBS-1.

RNAi resulted in a developmental delay phenotype in 97 % of the worms (515 out of 530 individuals tested). These animals reached the egg-laying adult stage no earlier than the 9th day after embryo hatching, in contrast with control worms, which reached

Table 1 Enzymatic and structural properties of purified CBS-1 variants

ND, not detected, Trp, tryptophan.

Protein	WT	K421A	E62K	CBS-1b
Catalytic activity (μmol · h^{-1} · mg^{-1})	1742 ± 259	0.41 ± 0.03	1663 ± 144	0.27 ± 0.05
Absorption ratio 280/412 nm	7.6	16.1	7.9	29.2
PLP absorption maximum (nm)	412	403 and 418	412	ND
Trp relative fluorescence	233	534	354	505
Trp fluorescence wavelength maximum (nm)	338	350	339	352
Relative delayed fluorescence	76	181	48	ND

the same stage on the 5th day of development. The affected larvae had a shorter body length than the controls (Supplementary Figure S8 at http://www.BiochemJ.org/bj/443/bj4430535add.htm). After RNAi of larvae, the most severe abnormalities were observed in the tissues that express the highest amount of CBS-1 (i.e. gut and pharynx; see the data above on the translational cbs-1–GFP vector). The gut cells of these animals showed reduced pigment granule birefringence under Nomarski optical microscopy (Supplementary Figure 8), and the anterior bulb of the pharynx exhibited abnormal morphology, with a balloon-like appearance and enlarged diameter (Supplementary Figure 8). These data show that CBS-1 is essential for normal development in nematodes.

We determined metabolic flux through the trans-sulfuration pathway by measuring homocysteine, cystathionine and cysteine concentrations in worm homogenates. To eliminate possible differences in metabolic fluxes in worms at various stages of development, the worms were collected at the latest larval developmental stage (L4). The homocysteine and cystathionine levels in *C. elegans* extracts were ~10× and ~1.6× higher in the knockdown strain than in the controls, whereas cysteine concentrations did not differ between the two strains (Figure 6). The observation of elevated homocysteine levels in CBS-1-knockdown worms

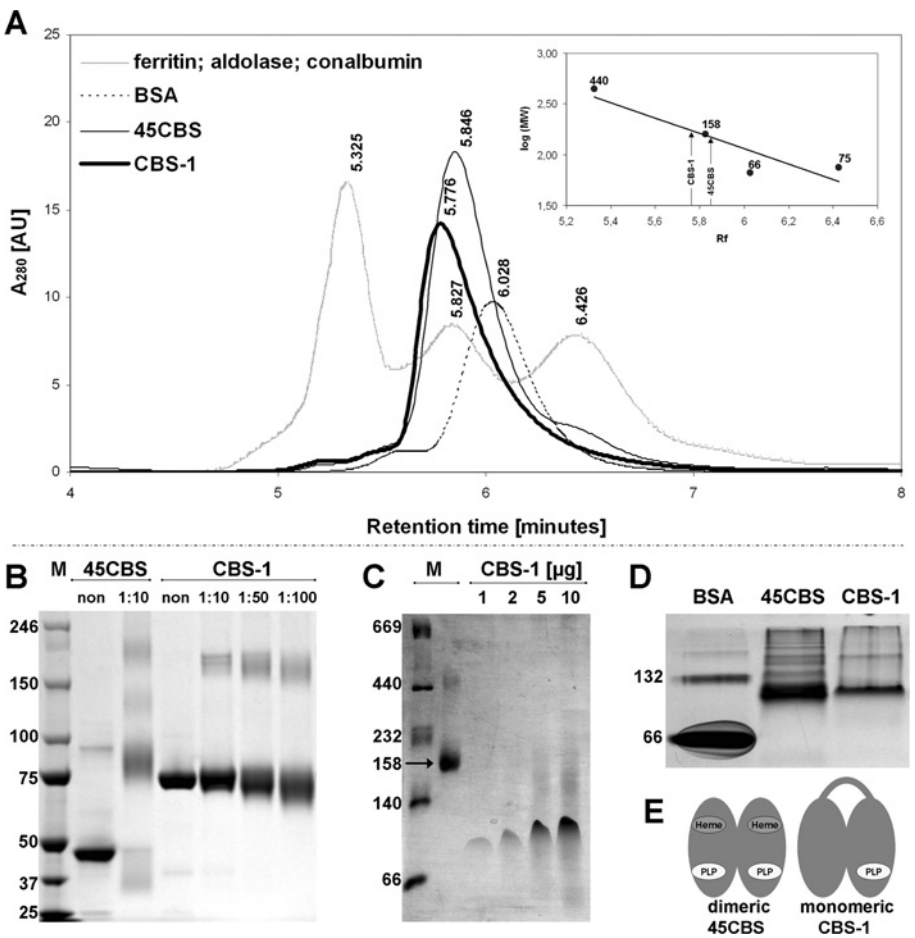

Figure 5 Determination of the quaternary structure of CBS-1

(**A**) SEC. The bold solid curve represents the elution profile of purified recombinant CBS-1, which has a retention time of 5.776 min and an estimated molecular mass of 168 kDa. The thin solid curve represents human 45CBS, which has a retention time of 5.846 min and an estimated molecular mass of 148 kDa. The dashed curve represents BSA with a retention time of 6.028. The grey (dotted) curve represents molecular standards eluted at the following retention times: ferritin (440 kDa), 5.325 min; aldolase (158 kDa), 5.827 min; and conalbumin (70 kDa), 6.426 min. AU, absorbance unit. (**B**) Cross-linking. Purified CBS-1 and human 45CBS were cross-linked with BS^3 in appropriate molar ratios of protein/modifier, as indicated in the Figure, and subjected to SDS/PAGE. In contrast with human 45CBS, which forms dimers, the mobility of CBS-1 does not change after cross-linking. (**C**) BN-PAGE. CBS-1, with a molecular mass of 78 kDa (four different amounts of loaded protein), migrates between molecular mass markers of 66 kDa and 140 kDa. The molecular protein mass markers include thyroglobulin (669 kDa), ferritin (440 kDa), catalase (232 kDa), lactate dehydrogenase (140 kDa), BSA (66 kDa) and aldolase (158 kDa). (**D**) Native PAGE. CBS-1, with a molecular mass of 78 kDa, migrates between molecular mass markers of 66 kDa and 132 kDa, similar to a ~90 kDa dimer of human 45CBS. In (**B**–**D**) the molecular mass is given in kDa on the left-hand side. M, marker. (**E**) Schematic diagram of the hypothetical quaternary structure of CBS-1 and comparison of its structure with that of human 45CBS.

Table 2 Stability and enzymatic properties of CBS-1 compared with human 45CBS

c_m, concentration of urea at which a fraction of folded proteins comprises 50 % of the entire protein population.

Protein	Nematode CBS-1	Human 45CBS
Oligomeric status	Monomer	Dimer
Michaelis constant K_m (mM)		
Serine	5.57 ± 0.68	2.20 ± 0.46†
Homocysteine	4.29 ± 0.97	0.33 ± 0.07†
Turnover number k_{cat} (s^{-1})		
Serine	48.12 ± 2.95	13.81 ± 0.88†
Homocysteine	43.31 ± 4.33	10.88 ± 0.72†
Catalytic efficiency k_{cat}/K_m ($mM^{-1} \cdot s^{-1}$)		
Serine	~8.5	~6
Homocysteine	~10	26.97 ± 5.87†
Characteristics of protein denaturation		
Midpoint of urea concentration c_m (M)	1.21 ± 0.02	4.08 ± 0.07*
Melting point T_m (°C)	41	51

*Value from Hnizda et al. [27].
†Value from Frank et al. [23].

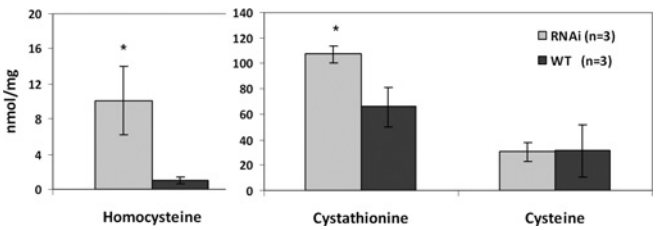

Figure 6 Metabolite levels in crude extracts of CBS-1-knockdown animals

The concentration of metabolites (in nanomoles per mg of protein) from RNAi and control experiments respectively. Homocysteine and cystathionine concentrations in CBS-1-deficient worms are significantly higher (10.1 and 107.1 nmol/mg of protein respectively) than in control worms (1.0 and 65.6 nmol/mg of protein respectively). Results are means $\pm$ S.D. from three independent experiments. *$P < 0.05$, as determined by Student's t test.

strongly supports an important role of this enzyme in maintaining homocysteine homoeostasis in *C. elegans*.

DISCUSSION

Evidence that CBS in *C. elegans* is encoded by *cbs-1*

In the present paper, we identified the *cbs-1* gene in *C. elegans*, which encodes an enzyme with cystathionine-synthesizing activity and is important for normal development of the nematode. Using a BLASTp search against a *C. elegans* protein database, we identified two nematode genes, *ZC373.1* and *F54A3.4*, that are highly homologous with CBS genes in other species. However, several lines of evidence demonstrate that only *ZC373.1* encodes a CBS, whereas *F54A3.4* is probably a pseudogene. The gene denoted *F54A3.4* has not been detected by RT–PCR, was not found by *in silico* searches in the appropriate EST and proteomic databases, and its partial deletion did not elicit biochemical or morphological phenotypic abnormalities. In contrast, *ZC373.1* mRNA has been detected by RT–PCR, its ESTs and peptides were annotated in appropriate databases, the enzyme was shown to be expressed endogenously in its entire length, and its knockdown resulted in severe biochemical and phenotypic consequences. Most importantly, the purified CBS-1 enzyme exhibited enzymatic properties consistent with previously characterized CBS enzymes from other species.

The unique domain architecture of nematode CBS enzymes

In silico analysis of the CBS-1 protein sequence showed that the CBS-1 of *C. elegans* possesses a unique multi-domain architecture that has not been reported previously for any other CBS. The unusual structure of CBS-1 includes the lack of a haem-binding region, the lack of a Bateman domain and the tandem arrangement of two conserved catalytic regions of which only the C-terminal region is catalytically active. Such a domain arrangement of predicted CBS enzymes in fully sequenced organisms has been found only in organisms from the nematode phylum, showing an evolutionarily divergent arrangement of the CBS protein in this phylum. Interestingly, the nematode *Loa loa* possesses a PLP-binding site in both CBS modules (Supplementary Figure S9 at http://www.BiochemJ.org/bj/443/bj4430535add.htm), suggesting that the unusual and unique structure of CBS enzymes in nematodes probably originates from a duplication of the conserved catalytic region in a common ancestor followed by mutations abolishing PLP binding in the N-terminal module.

To our knowledge there is no evidence, except of nematode CBS proteins, regarding fold-type II PLP-dependent proteins lacking a PLP-binding site. Thus the function, if any, of the N-terminal module in the nematode CBS-1 protein remains unclear. Several pieces of experimental evidence obtained in the present study clearly show that this module does not have canonical catalytic function. We speculate that mutations in this portion of the nematode CBS enzyme may have permitted the acquisition of novel structural and functional properties, such as changes in protein stability and folding, protein–protein interactions, or regulation of enzyme activity. Studies of truncated variants suggest that the N-terminal module may be important for proper folding and subsequent stability of CBS-1 (see above). Because CBS-1 forms a monomer, it is probable that its N-terminal and C-terminal modules interact to form a structure similar to that of the human 45CBS dimer. However, the proposed interdomain interaction cannot be sufficiently supported by the computational modelling procedures using previously solved crystal structures of CBS proteins, and thus it requires further study of the three-dimensional spatial arrangement of CBS-1 at atomic resolution. The N-terminal module of CBS-1 may also have a regulatory role. The existence of tandem duplicated conserved modules of which only one is catalytically active in a single polypeptide is similar to the well-known case of tyrosine protein kinases [JAKs (Janus kinases)]. In tandem with a catalytically active kinase domain, these kinases have a catalytically inactive pseudo-kinase domain that has been implicated in the regulation of their activity [36]. Alternatively, the N-terminal module of CBS-1 may also play a role in protein–protein interactions, such as the interactions with the SUMOylation enzyme apparatus or huntingtin that have been described for human and rodent CBS-1 orthologues respectively [37,38].

More intriguingly, expression of the spliced variant *cbs-1b* shows that the N-terminal module of CBS-1 can be produced *in vivo* without the catalytic C-terminal module. This finding suggests that the non-catalytic module may play a role in additional biological processes independent of the catalytic module. However, it should be noted that misspliced variants with premature stop codons are commonly targeted by a cellular RNA nonsense-mediated decay mechanism [39]; therefore, the existence of a separate nematode N-terminal domain *in vivo* should be investigated in future studies.

Possible biological roles of CBS-1 enzymatic activity in *C. elegans*

Because *cbs-1* is expressed in a limited number of tissues, it is tempting to speculate on the role of this enzyme in the organs

in which it is expressed. High expression of *cbs-1* was observed throughout post-embryonic development in the intestine, which is characterized by secretion of digestive enzymes and high metabolic activity in *C. elegans*, such as the synthesis and storage of macromolecules and detoxification of xenobiotics [40]. Thus the expression of *cbs-1* in *C. elegans* intestine may mirror the high expression of CBS in the mammalian liver, pancreas and small intestine, in which CBS plays an important role in homocysteine homoeostasis and/or in the provision of cysteine for glutathione production [41]. We hypothesize that the intestinal expression of *cbs-1* in worms may serve similar purposes, namely removal of homocysteine or cysteine biosynthesis.

Expression of *cbs-1* has also been observed in pharyngeal muscles and hypodermis. Because neither of these tissues shows high metabolic activity compared with the intestine, there are other possible explanations for CBS-1 activity in these tissues. Because both hypodermal cells and pharyngeal muscle cells secrete cuticle (http://www.wormatlas.org/), we propose that CBS-1 may provide cysteine, which is important for cuticle formation and its stabilization by disulfide bonds [42]. Another possible role for CBS-1 in muscle and hypodermis is the production of the neuromodulator and smooth muscle relaxant hydrogen sulfide [43]. The endogenous biosynthesis of H_2S via CBS might serve for smooth muscle relaxation in the strongly innervated nematode pharynx or in regulating the expression of HIF-1 (hypoxia-inducible factor 1) target genes in the hypodermis [44]. Interestingly, although CBS is thought to be the main enzyme that produces hydrogen sulfide in the mammalian brain [45], we did not observe a GFP signal in neurons. This finding suggests that the endogenous production of hydrogen sulfide in *C. elegans* neurons is mediated by different enzymes than in other species or that the role of hydrogen sulfide in *C. elegans* neurons is negligible.

C. elegans as a model of CBS deficiency

Because many genes implicated in human diseases are well-conserved across phyla [46], *C. elegans* is considered by many investigators to be a suitable model for studying cellular and metabolic mechanisms in selected genetic disorders [47–49]. In addition to its low cost of maintenance and short generation time, other advantages of the *C. elegans* model include the possibility of observing cellular processes *in vivo* and of easily screening for the effects of novel therapies [50,51]. In the present study, we examined the morphological and biochemical effects of nematode CBS-1 deficiency. These effects may in part recapitulate the human disease homocystinuria, which results from CBS deficiency. Homocystinuria is characterized by increased tissue, plasma and urinary concentrations of homocysteine, and by decreased concentrations of cystathionine and cysteine [52,53]. Its clinical features include liver steatosis, connective tissue disorder, thromboembolism and various degrees of central nervous system involvement [53]. In our CBS-1–GFP localization study, CBS-1-knockdown worms exhibited abnormal morphology of several tissues that express the *cbs-1* gene. Using light microscopy, we observed a reduced birefringent signal from pigment gut granules, which are considered to be lysosome-related organelles [54]. Although the function and composition of these granules has not been fully elucidated, the abnormal pattern of gut granules in CBS-1-knockdown animals may in part correspond to the liver steatosis observed in murine and human CBS deficiency. Furthermore, the observed abnormal pharyngeal morphology of CBS-1-deficient worms may possibly correspond to some of the neurological sequelae of human CBS deficiency. It appears that the CBS-knockdown nematodes produced in the present study may in part recapitulate some of the features of human homocystinuria due to CBS deficiency.

In the CBS-1-deficient nematodes produced in the present study, the amounts of CBS-1 antigen and enzyme activity decreased to ~10–15 % those of WT worms. This degree of enzyme deficiency resulted in an approximately 10-fold increase in homocysteine concentrations in worm extracts compared with the WT strain, demonstrating an essential role for CBS-1 in maintaining homocysteine homoeostasis in *C. elegans*. Because exposure of worms to homocysteine in medium [55] leads to a similar developmental delay as the *cbs-1* RNAi in the present study, it is conceivable that high tissue levels of homocysteine may be directly responsible for the developmental delay phenotype that we observed. Surprisingly, and in contrast with human patients with CBS deficiency [53], cystathionine levels in CBS-1-deficient worms were only slightly increased. However, a similar elevation in plasma cystathionine was reported for one murine model of CBS deficiency [56]. We hypothesize that elevated cystathionine in CBS-1-deficient worms may be caused by three possible mechanisms: (i) elevated homocysteine may inactivate CGL, as proposed previously for a murine model of CBS deficiency [56]; (ii) elevated homocysteine may lead to formation of cystathionine via condensation of cysteine and homocysteine by CGL [57]; and (iii) cystathionine may be synthesized by a hypothetical cystathionine γ-synthase in the reverse trans-sulfuration pathway using cysteine and *O*-succinylhomoserine. Moreover, the CBS-1-deficient worms observed in the present study did not exhibit cysteine depletion, which is a common feature of human CBS deficiency. We hypothesize that cysteine levels in deficient worms are maintained by sufficient cysteine intake from *E. coli* or by biosynthesis of cysteine via a hypothetical sulfur assimilation pathway because *C. elegans* possesses several bacterial and plant cysteine synthase homologues (see above, [58]).

AUTHOR CONTRIBUTION

Roman Vozdek designed and performed most of the experiments and wrote the first draft of the paper; Aleš Hnízda purified and further characterized recombinant CBS-1; Jakub Krijt measured aminothiols and cystathionine by HPLC and LC–MS/MS in the appropriate studies; Marta Kostrouchová co-ordinated the experiments with *C. elegans*; and Viktor Kožich co-ordinated the whole project. All authors have extensively revised various versions of the paper and approved its final version prior to submission.

ACKNOWLEDGEMENTS

We thank Dr A. Fire for vector pPD95.75, and Eva Zouharová, Mrs Kateřina Raková, Hana Prouzová, Jitka Honzíková and Professor Milan Kodíček for technical assistance and advice.

FUNDING

This work was supported by a Wellcome Trust International Senior Research Fellowship in Biomedical Science in Central Europe [number 070255/Z/03/Z], the Grant Agency of the Charles University in Prague [grant numbers 21709 and SVV262502], the Ministry of Education of the Czech Republic [grant number MSM0021620806] and the Czech Science Foundation [grant number 304/08/0970].

REFERENCES

1 Finkelstein, J. D. (1998) The metabolism of homocysteine: pathways and regulation. Eur. J. Pediatr. **157**, S40–S44

1a Taoka, S., Ohja, S., Shan, X., Kruger, W. D. and Banerjee, R. (1998) Evidence for heme-mediated redox regulation of human cystathionine beta-synthase activity. J. Biol. Chem. **273**, 25179–25184

2 Banerjee, R. and Zou, C. G. (2005) Redox regulation and reaction mechanism of human cystathionine-beta-synthase: a PLP-dependent hemesensor protein. Arch. Biochem. Biophys. **433**, 144–156

3 Cherney, M. M., Pazicni, S., Frank, N., Marvin, K. A., Kraus, J. P. and Burstyn, J. N. (2007) Ferrous human cystathionine beta-synthase loses activity during enzyme assay due to a ligand switch process. Biochemistry **46**, 13199–13210
4 Smith, A. T., Majtan, T., Freeman, K. M., Su, Y., Kraus, J. P. and Burstyn, J. N. (2011) Cobalt cystathionine beta-synthase: a cobalt-substituted heme protein with a unique thiolate ligation motif. Inorg. Chem. **50**, 4417–4427
5 Mehta, P. K. and Christen, P. (2000) The molecular evolution of pyridoxal-5′-phosphate-dependent enzymes. Adv. Enzymol. Relat. Areas Mol. Biol. **74**, 129–184
6 Kery, V., Poneleit, L. and Kraus, J. P. (1998) Trypsin cleavage of human cystathionine beta-synthase into an evolutionarily conserved active core: structural and functional consequences. Arch. Biochem. Biophys. **355**, 222–232
7 Taoka, S., Widjaja, L. and Banerjee, R. (1999) Assignment of enzymatic functions to specific regions of the PLP-dependent heme protein cystathionine beta-synthase. Biochemistry **38**, 13155–13161
8 Skovby, F., Kraus, J. P. and Rosenberg, L. E. (1984) Biosynthesis and proteolytic activation of cystathionine beta-synthase in rat liver. J. Biol. Chem. **259**, 588–593
9 Zou, C. G. and Banerjee, R. (2003) Tumor necrosis factor-α-induced targeted proteolysis of cystathionine beta-synthase modulates redox homeostasis. J. Biol. Chem. **278**, 16802–16808
10 Jhee, K. H., McPhie, P. and Miles, E. W. (2000) Yeast cystathionine beta-synthase is a pyridoxal phosphate enzyme but, unlike the human enzyme, is not a heme protein. J. Biol. Chem. **275**, 11541–11544
11 Nozaki, T., Shigeta, Y., Saito-Nakano, Y., Imada, M. and Kruger, W. D. (2001) Characterization of transsulfuration and cysteine biosynthetic pathways in the protozoan hemoflagellate, *Trypanosoma cruzi*. Isolation and molecular characterization of cystathionine beta-synthase and serine acetyltransferase from Trypanosoma. J. Biol. Chem. **276**, 6516–6523
12 Koutmos, M., Kabil, O., Smith, J. L. and Banerjee, R. (2010) Structural basis for substrate activation and regulation by cystathionine beta-synthase (CBS) domains in cystathionine beta-synthase. Proc. Natl. Acad. Sci. U.S.A. **107**, 20958–20963
13 Jhee, K. H., McPhie, P. and Miles, E. W. (2000) Domain architecture of the heme-independent yeast cystathionine beta-synthase provides insights into mechanisms of catalysis and regulation. Biochemistry **39**, 10548–10556
14 Brenner, S. (1974) The genetics of *Caenorhabditis elegans*. Genetics **77**, 71–94
15 Meier, M., Janosik, M., Kery, V., Kraus, J. P. and Burkhard, P. (2001) Structure of human cystathionine beta-synthase: a unique pyridoxal 5′-phosphate-dependent heme protein. EMBO J. **20**, 3910–3916
16 Wiederstein, M. and Sippl, M. J. (2007) ProSA-web: interactive web service for the recognition of errors in three-dimensional structures of proteins. Nucleic Acids Res. **35**, W407–W410
17 Guex, N. and Peitsch, M. C. (1997) SWISS-MODEL and the Swiss-PdbViewer: an environment for comparative protein modeling. Electrophoresis **18**, 2714–2723
18 Neron, B., Menager, H., Maufrais, C., Joly, N., Maupetit, J., Letort, S., Carrere, S., Tuffery, P. and Letondal, C. (2009) Mobyle: a new full web bioinformatics framework. Bioinformatics **25**, 3005–3011
19 Chenna, R., Sugawara, H., Koike, T., Lopez, R., Gibson, T. J., Higgins, D. G. and Thompson, J. D. (2003) Multiple sequence alignment with the Clustal series of programs. Nucleic Acids Res. **31**, 3497–3500
20 Guindon, S. and Gascuel, O. (2003) A simple, fast, and accurate algorithm to estimate large phylogenies by maximum likelihood. Syst. Biol. **52**, 696–704
21 Huson, D. H., Richter, D. C., Rausch, C., Dezulian, T., Franz, M. and Rupp, R. (2007) Dendroscope: an interactive viewer for large phylogenetic trees. BMC Bioinf. **8**, 460
22 Boulin, T., Etchberger, J. F. and Hobert, O. (2006) Reporter gene fusions. In WormBook (The *C. elegans* Research Community, ed.), pp. 1–23, doi/10.1895/wormbook.1.106.1
23 Frank, N., Kent, J. O., Meier, M. and Kraus, J. P. (2008) Purification and characterization of the wild type and truncated human cystathionine beta-synthase enzymes expressed in *E. coli*. Arch. Biochem. Biophys. **470**, 64–72
24 Janosik, M., Meier, M., Kery, V., Oliveriusova, J., Burkhard, P. and Kraus, J. P. (2001) Crystallization and preliminary X-ray diffraction analysis of the active core of human recombinant cystathionine beta-synthase: an enzyme involved in vascular disease. Acta Crystallogr. Sect. D Biol. Crystallogr. **57**, 289–291
25 Laemmli, U. K. (1970) Cleavage of structural proteins during the assembly of the head of bacteriophage T4. Nature **227**, 680–685
26 Wittig, I., Braun, H. P. and Schagger, H. (2006) Blue native PAGE. Nat. Protoc. **1**, 418–428
27 Hnizda, A., Spiwok, V., Jurga, V., Kozich, V., Kodicek, M. and Kraus, J. P. (2010) Cross-talk between the catalytic core and the regulatory domain in cystathionine beta-synthase: study by differential covalent labeling and computational modeling. Biochemistry **49**, 10526–10534
28 Maclean, K. N., Sikora, J., Kozich, V., Jiang, H., Greiner, L. S., Kraus, E., Krijt, J., Crnic, L. S., Allen, R. H., Stabler, S. P. et al. (2010) Cystathionine beta-synthase null homocystinuric mice fail to exhibit altered hemostasis or lowering of plasma homocysteine in response to betaine treatment. Mol. Genet. Metab. **101**, 163–171
29 Krijt, J., Kopecka, J., Hnizda, A., Moat, S., Kluijtmans, L. A., Mayne, P. and Kozich, V. (2011) Determination of cystathionine beta-synthase activity in human plasma by LC–MS/MS: potential use in diagnosis of CBS deficiency. J. Inherited Metab. Dis. **34**, 49–55
30 Mello, C. and Fire, A. (1995) DNA transformation. Methods Cell Biol. **48**, 451–482
31 Janosik, M., Oliveriusova, J., Janosikova, B., Sokolova, J., Kraus, E., Kraus, J. P. and Kozich, V. (2001) Impaired heme binding and aggregation of mutant cystathionine beta-synthase subunits in homocystinuria. Am. J. Hum. Genet. **68**, 1506–1513
32 Schrimpf, S. P., Weiss, M., Reiter, L., Ahrens, C. H., Jovanovic, M., Malmstrom, J., Brunner, E., Mohanty, S., Lercher, M. J., Hunziker, P. E. et al. (2009) Comparative functional analysis of the *Caenorhabditis elegans* and *Drosophila melanogaster* proteomes. PLoS Biol. **7**, e48
33 McKay, S. J., Johnsen, R., Khattra, J., Asano, J., Baillie, D. L., Chan, S., Dube, N., Fang, L., Goszczynski, B., Ha, E. et al. (2003) Gene expression profiling of cells, tissues, and developmental stages of the nematode *C. elegans*. Cold Spring Harb. Symp. Quant. Biol. **68**, 159–169
34 Rege, V. D., Kredich, N. M., Tai, C. H., Karsten, W. E., Schnackerz, K. D. and Cook, P. F. (1996) A change in the internal aldimine lysine (K42) in *O*-acetylserine sulfhydrylase to alanine indicates its importance in transimination and as a general base catalyst. Biochemistry **35**, 13485–13493
35 Belew, M. S., Quazi, F. I., Willmore, W. G. and Aitken, S. M. (2009) Kinetic characterization of recombinant human cystathionine beta-synthase purified from *E. coli*. Protein Expression Purif. **64**, 139–145
36 Aringer, M., Cheng, A., Nelson, J. W., Chen, M., Sudarshan, C., Zhou, Y. J. and O'Shea, J. J. (1999) Janus kinases and their role in growth and disease. Life Sci. **64**, 2173–2186
37 Kabil, O., Zhou, Y. and Banerjee, R. (2006) Human cystathionine beta-synthase is a target for sumoylation. Biochemistry **45**, 13528–13536
38 Boutell, J. M., Wood, J. D., Harper, P. S. and Jones, A. L. (1998) Huntingtin interacts with cystathionine beta-synthase. Hum. Mol. Genet. **7**, 371–378
39 Zahler, A. M. (2005) Alternative splicing in *C. elegans*. In WormBook (The *C. elegans* Research Community, ed.), pp. 1–13, doi/10.1895/wormbook.1.31.1
40 McGhee, J. D. (2007) The *C. elegans* intestine. In WormBook (The *C. elegans* Research Community, ed.). pp. 1–36, doi/10.1895/wormbook.1.133.1
41 Finkelstein, J. D. (2000) Pathways and regulation of homocysteine metabolism in mammals. Semin. Thromb. Hemostasis **26**, 219–225
42 Page, A. P. and Johnstone, I. L. (2007) The cuticle. In WormBook (The *C. elegans* Research Community, ed.). pp. 1–15, doi/10.1895/wormbook.1.138.1
43 Kimura, H. (2011) Hydrogen sulfide: its production, release and functions. Amino Acids **41**, 113–121
44 Budde, M. W. and Roth, M. B. (2010) Hydrogen sulfide increases hypoxia-inducible factor-1 activity independently of von Hippel–Lindau tumor suppressor-1 in *C. elegans*. Mol. Biol. Cell **21**, 212–217
45 Abe, K. and Kimura, H. (1996) The possible role of hydrogen sulfide as an endogenous neuromodulator. J. Neurosci. **16**, 1066–1071
46 Kuwabara, P. E. and O'Neil, N. (2001) The use of functional genomics in *C. elegans* for studying human development and disease. J. Inherited Metab. Dis. **24**, 127–138
47 Chandler, R. J., Aswani, V., Tsai, M. S., Falk, M., Wehrli, N., Stabler, S., Allen, R., Sedensky, M., Kazazian, H. H. and Venditti, C. P. (2006) Propionyl-CoA and adenosylcobalamin metabolism in *Caenorhabditis elegans*: evidence for a role of methylmalonyl-CoA epimerase in intermediary metabolism. Mol. Genet. Metab. **89**, 64–73
48 Calvo, A. C., Pey, A. L., Ying, M., Loer, C. M. and Martinez, A. (2008) Anabolic function of phenylalanine hydroxylase in *Caenorhabditis elegans*. FASEB J. **22**, 3046–3058
49 Fisher, A. L., Page, K. E., Lithgow, G. J. and Nash, L. (2008) The *Caenorhabditis elegans K10C2.4* gene encodes a member of the fumarylacetoacetate hydrolase family: a *Caenorhabditis elegans* model of type I tyrosinemia. J. Biol. Chem. **283**, 9127–9135
50 Link, E. M., Hardiman, G., Sluder, A. E., Johnson, C. D. and Liu, L. X. (2000) Therapeutic target discovery using *Caenorhabditis elegans*. Pharmacogenomics **1**, 203–217
51 Kaletta, T. and Hengartner, M. O. (2006) Finding function in novel targets: *C. elegans* as a model organism. Nat. Rev. **5**, 387–398
52 Kraus, J. P., Janosik, M., Kozich, V., Mandell, R., Shih, V., Sperandeo, M. P., Sebastio, G., de Franchis, R., Andria, G., Kluijtmans, L. A. et al. (1999) Cystathionine beta-synthase mutations in homocystinuria. Hum. Mutat. **13**, 362–375
53 Kraus, J. P. and Kožich, V. (2001) Cystathionine-β-synthase and its deficiency. In Homocysteine in Health and Disease (Carmel, R. and Jacobsen, D. W., eds), pp. 223–243, Cambridge University Press, Cambridge
54 Hermann, G. J., Schroeder, L. K., Hieb, C. A., Kershner, A. M., Rabbitts, B. M., Fonarev, P., Grant, B. D. and Priess, J. R. (2005) Genetic analysis of lysosomal trafficking in *Caenorhabditis elegans*. Mol. Biol. Cell **16**, 3273–3288
55 Khare, S., Gomez, T., Linster, C. L. and Clarke, S. G. (2009) Defective responses to oxidative stress in protein l-isoaspartyl repair-deficient *Caenorhabditis elegans*. Mech. Ageing Dev. **130**, 670–680

56 Maclean, K. N., Sikora, J., Kozich, V., Jiang, H., Greiner, L. S., Kraus, E., Krijt, J., Overdier, K. H., Collard, R., Brodsky, G. L. et al. (2010) A novel transgenic mouse model of CBS-deficient homocystinuria does not incur hepatic steatosis or fibrosis and exhibits a hypercoagulative phenotype that is ameliorated by betaine treatment. Mol. Genet. Metab. **101**, 153–162

57 Singh, S., Padovani, D., Leslie, R. A., Chiku, T. and Banerjee, R. (2009) Relative contributions of cystathionine beta-synthase and gamma-cystathionase to H2S biogenesis via alternative trans-sulfuration reactions. J. Biol. Chem. **284**, 22457–22466

58 Budde, M. W. and Roth, M. B. (2011) The response of *Caenorhabditis elegans* to hydrogen sulfide and hydrogen cyanide. Genetics **189**, 521–532

Received 15 August 2011/13 December 2011; accepted 13 January 2012
Published as BJ Immediate Publication 13 January 2012, doi:10.1042/BJ20111478

Biochem. J. (2012) **443**, 535–547 (Printed in Great Britain) doi:10.1042/BJ20111478

online data

SUPPLEMENTARY ONLINE DATA

Novel structural arrangement of nematode cystathionine β-synthases: characterization of *Caenorhabditis elegans* CBS-1

Roman VOZDEK, Aleš HNÍZDA, Jakub KRIJT, Marta KOSTROUCHOVÁ and Viktor KOŽICH[1]

Institute of Inherited Metabolic Disorders, Charles University in Prague, First Faculty of Medicine and General University Hospital, Ke Karlovu 2, 128 08, Praha 2, Czech Republic

Figure S1 Unrooted tree of fold-type II PLP-dependent proteins with ten CBS homologues in *C. elegans*

For phylogenetic analysis, we used various proteins from the family of fold-type II PLP-dependent proteins: CBS_Human (UniProt entry P35520), CBS_Rat (UniProt entry P32232), CBS_Drosophila (UniProt entry Q9VRD9), CBS_Trypanosoma (UniProt entry Q9BH24), CBS_Saccharomyces (UniProt entry P32582), CYSK_Saccharomyces (UniProt entry P53206) CYSK_Arabidopsis (UniProt entry P47998), CYSM_E. coli (UniProt entry P16703), CYSK_E. coli (UniProt entry P0ABK5), SDSL_Human (UniProt entry Q96GA7), THDH_Saccharomyces (UniProt entry P00927), THD1_E. coli (UniProt entry P04968) and THD1_Arabidopsis (UniProt entry Q9ZSS6). Ten CBS homologues (bold font) are presented in Table S1. The numbers at the internal nodes represent bootstrapped values (maximum 100). The upper left-hand edge in red denotes the CBS branch. The tree topology demonstrates three separated groups for ten CBS homologues in *C. elegans*: ZC373.1 and F54A3.4 belong to the CBS branch, C17G1.7, R08E5.2, F59A7.9 and K10H10.2 belong to the cysteine synthase A branch, and the remaining homologues belong to other fold-type II PLP-dependent protein families. CYSK, cysteine synthase A; CYSM, cysteine synthase B; SDSL/THD, serine/threonine dehydratase family.

[1] To whom correspondence should be addressed (email Viktor.Kozich@LF1.cuni.cz).

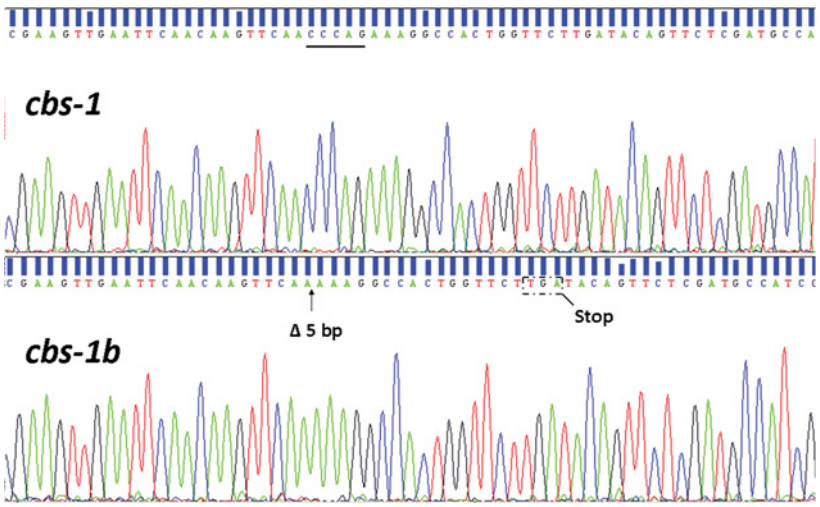

Figure S2 Sequences of *cbs*-1 RT–PCR products covering the exon 6 and 7 junction

Two splice variants of *cbs-1* were found. The novel *cbs-1b* transcript leads to a frameshift and a subsequent stop codon that allows for translation of the separated N-terminal module of CBS-1.

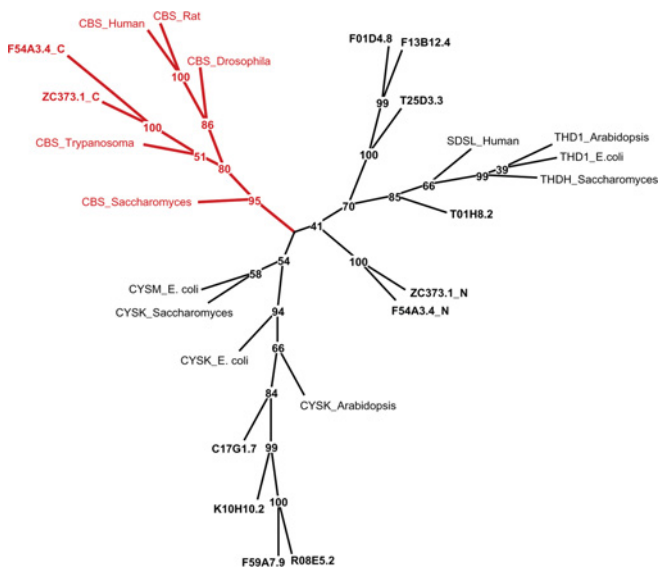

Figure S3 Unrooted tree of separated conserved regions from CBS-1 with various fold-type II PLP-dependent proteins

This tree is taken from the same phylogenetic study as that presented in Figure S1, with the exception that the two conserved regions from CBS orthologues ZC373.1 and F54A3.4, were separated for the analysis. The topology of the unrooted tree demonstrates that the N-terminal regions of CBS homologues (ZC373.1_N and F54A3.4_N) do not belong to any branch containing the analysed proteins, whereas the C-terminal regions (ZC373.1_C and F54A3.4_C) belong to the CBS branch. Alignment of the N-terminal module of *C. elegans* CBS-1 (the first of the two tandemly arranged regions, i.e. residues 14–322) revealed 29 % identity and an e-value of 5e − 27 compared with the catalytic core of human CBS (residues 72–397), whereas the C-terminal module (i.e. residues 374–702 of CBS-1) revealed much higher 54 % identity and an e-value of 2e − 99.

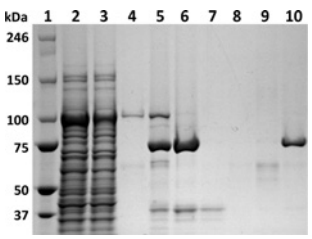

Figure S4 CBS-1 purification procedure

The purification procedure for CBS-1 is illustrated by a 3–8 % SDS-containing polyacrylamide gel stained with Coomassie EZ Blue. Lane 1, molecular mass markers; lane 2, bacterial extract after centrifugation; lane 3, flow-through fraction from glutathione–Sepharose column; 4, wash fraction of glutathione–Sepharose column; lane 5, fusion protein that was cleaved by PreScission protease; lane 6, elution of CBS-1 after on-column cleavage; lane 7, flow-through fraction from the Ni-Sepharose column; lanes 8 and 9, wash fractions of the Ni-Sepharose column by IMAC buffer containing 20 mM and 50 mM imidazole respectively; lane 10, elution of CBS-1 by IMAC buffer containing 75 mM imidazole. The molecular mass is given in kDa on the left-hand side.

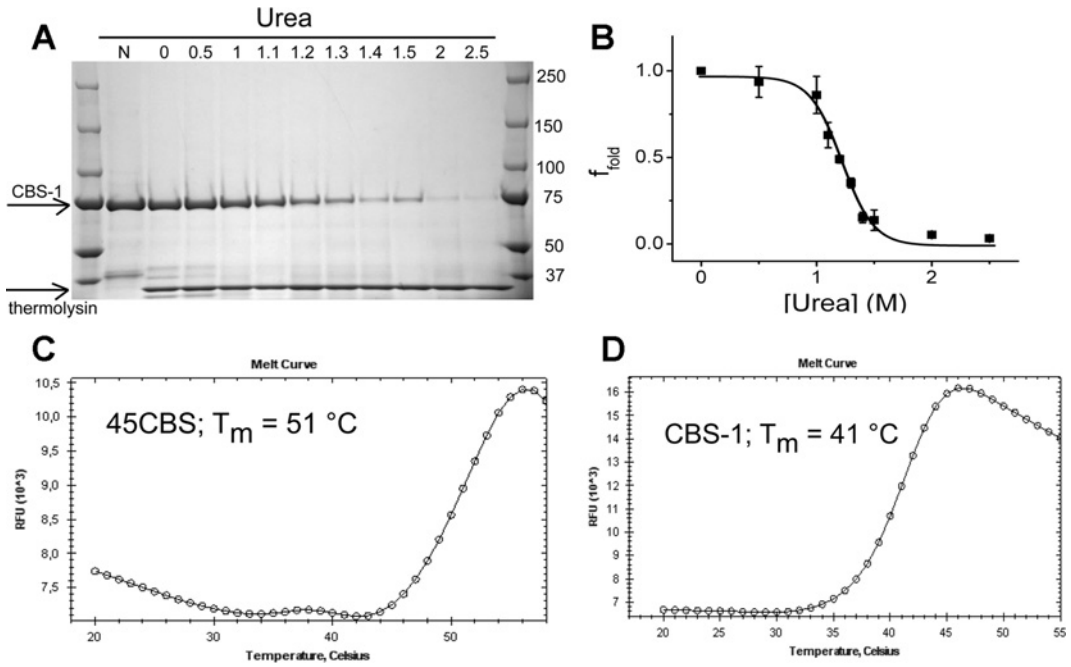

Figure S5 Pulse proteolysis and fluorescence-based thermal-shift assay

Pulse proteolysis in a urea gradient employing thermolysin and thermal-based assays were used to determine possible differences in enzyme stability between CBS-1 and human 45CBS. (**A**) Representative SDS/PAGE gel. The molar concentration of urea for the proteolytic pulse is indicated at the top of each lane and the molecular mass is given in kDa on the right-hand side. (**B**) F-fold values, which represent the fraction of the remaining intact protein after the proteolytic pulse, are plotted against the urea concentration. Results are means ± S.D. from three measurements and the curves were fitted by non-linear regression. (**C** and **D**) Melting curves in fluorescence-based thermal shift assays reveal melting points (T_m) of 51 °C and 41 °C for human 45CBS and CBS-1 respectively.

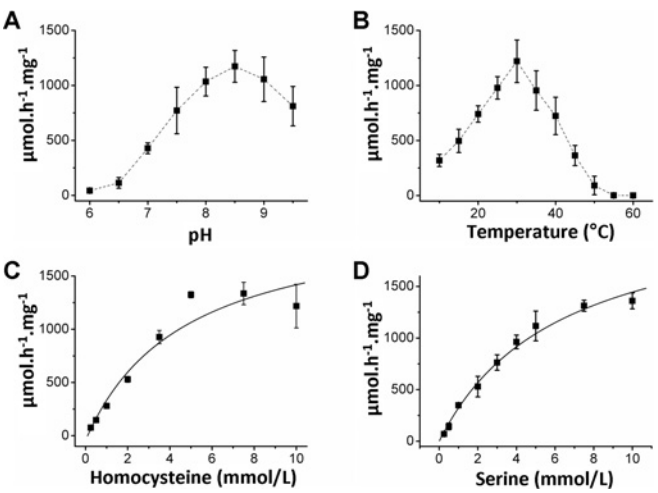

Figure S6 Enzymatic properties of recombinant CBS-1

(**A** and **B**) The dependence of CBS activity on pH and temperature respectively. The kinetic properties of CBS-1 for 1–10 mM homocysteine in a mixture with 10 mM serine are shown in (**C**), whereas the properties for 1–10 mM serine in a mixture with 10 mM homocysteine are shown in (**D**). Results are means ± S.D. from four measurements.

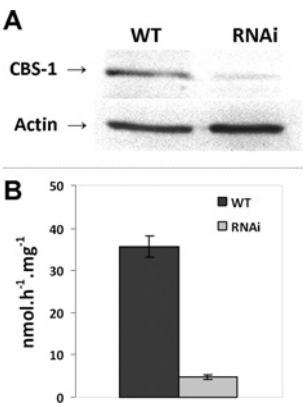

Figure S7 Western blot analysis and CBS assay of crude nematode extracts

(**A**) Western blot analysis showing a decreased level of CBS-1 protein in nematodes after RNAi. Actin was used as a reference protein. (**B**) CBS activity is significantly decreased in nematodes after RNAi. Results are means ± S.D. from two independent measurements.

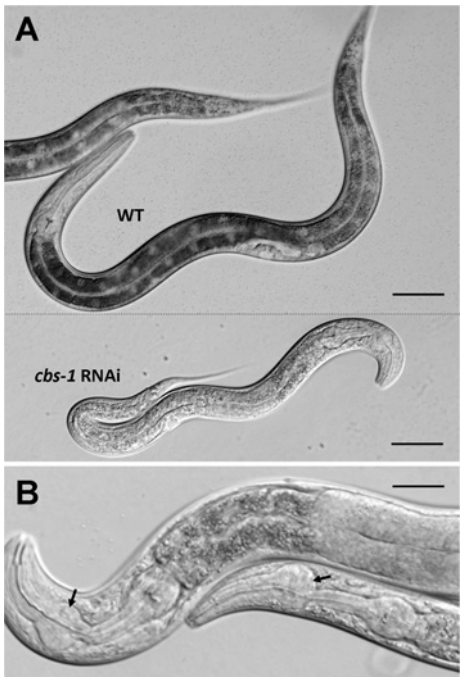

Figure S8 Inhibition of *cbs-1* by RNAi

Images show the body morphologies of worms in Nomarski optics. (**A**) L4 stage of *cbs-1* RNAi and WT worms. The affected worms exhibit decreased body mass and partial lack of pigment granules in the intestine. Scale bars, 50 μm. (**B**) Higher magnification of an affected adult nematode pharynx. The pharynx shows abnormal morphogenesis of the metacorpus with a balloon-like appearance indicated by an arrow. Scale bar, 25 μm.

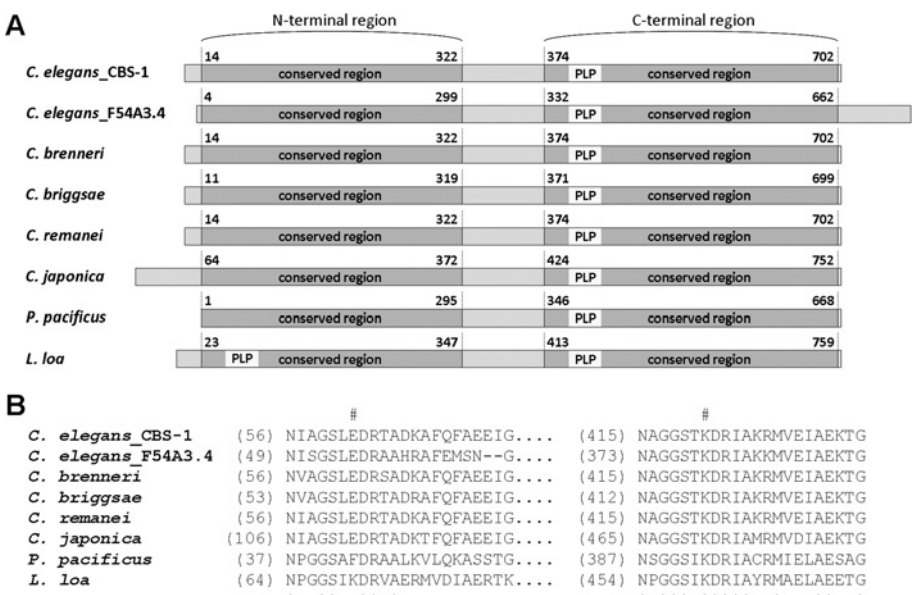

Figure S9 Domain architecture of CBS enzymes in nematodes

(**A**) Domain organization of nematode CBSs. The predicted amino acid sequences of hypothetical nematode CBSs were aligned with the sequence of *C. elegans* CBS-1, and the domain architecture of the proteins was inferred from the degree of homology. Primary structures are aligned by the PLP-binding lysine residue. The numbers indicate the first and the last amino acid residues in each of the conserved domains. Hypothetical proteins included in the alignment are as follows: *C. elegans*_ZC373.1 (CBS-1, UniProt entry Q23264); *C. brenneri* (WormBase accession number CN28558); *C. briggsae* (UniProt entry A8WRM3); *C. remanei* (UniProt entry E3MMP8); *C. japonica* (WormBase accession number JA15528); *C. elegans* F54A3.4 (UniProt entry Q9N4K2); *Pristionchus pacificus* (WormBase accession number PP12619); *Loa loa* (UniProt entry E1FTU4). (**B**) Amino acid alignment of hypothetical PLP-binding site of separated N-terminal and C-terminal conserved regions of various nematode CBSs. #, site of the putative PLP-binding lysine residues. $*$, conserved residue. Only *Loa loa* CBS contains a lysine residue in both PLP-binding sites.

Table S1 Primer sequences

Primers A–F were used to generate the cbs-1–GFP vector (see the GFP reporter assay section of the main text), G and H were used for the amplification of the shortened *cbs-1* coding sequence (see the RNA-mediated interference section of the main text), I–K (sense) and L–O (antisense) were used in combination to amplify the *F54A3.4* open reading frame (see the PCR amplification and sequencing section of the main text), P–U (sense) and V (antisense) were used for the amplification of the *cbs-1* coding sequence with specific cloning overhangs (see the Bacterial expression and purification section of the main text). Primers W–Z were used for site-directed mutagenesis.

Primer	Sequence
A, cbs-1_S	5′-ACTTGACGGAAAAGCTGGCAGA-3′
B, cbs-1_A	5′-AGTCGACCTGCAGGCATGCAAGCTGGCGTCTAGGAAATGACGCTCATTC-3′
C, GFP_S	5′-AGCTTGCATGCCTGCAGGTCG-3′
D, GFP_AS	5′-AAGGGCCCGTACGGCCGACTA-3′
E, cbs-1_S*	5′-GAGGAATGACCATCAATTTGA-3′
F, GFP_AS*	5′-GGAAACAGTTATGTTTGGTATA-3′
G , RNAi_S	5′-GACCCTCATGGATCTATTC-3′
H, RNAi_AS	5′-GACGCTCATTCATCCAATC-3′
I, F54_S1	5′-GACGAATTCATGTGCCTGCCTACCATTAAA-3′
J, F54_S2	5′-GGCAAGACGCCACTGGTGAA-3′
K, F54_S3	5′-AGAAGACAACAGTGGTCGGAGTGAGAT-3′
L, F54_AS1	5′-CAAGCGGCCGCTCAATAGAAAATGCGAGAGCG-3′
M, F54_AS2	5′-AGAGATTCCGGTGATGGTAC-3′
N, F54_AS3	5′-CAACGGCACCAGTTGAGTTG-3′
O, F54_AS4	5′-TGGCTTCCAGCACTGCCGC-3′
P, CBS-1_S	5′-CCTGGGATCCATGATCCAAAACGAAGTTTCC-3′
Q, Δ1–372	5′-CCTGGGATCCCCAGAAAGGCCACTGGTTCTT-3′
R, Δ1–322	5′-CCTGGGATCCGTGGTGACCAGAAAAGATGGA-3′
S, Δ1–299	5′-CCTGGGATCCATGGAATTAGAAATTATC-3′
T, b/375	5′-CCTGGGATCCATGGACCACAACCAAACAGCA-3′
U, b/360	5′-CCTGGGATCCATGATCCAACTAAACTTGCTG-3′
V, CBS-1_AS	5′-GCCGCTCGAGTTAGTGGTGATGGTGATGATGGGCGTCTAGGAAATGACG-3′
W, K421A_S	5′-TGAACGCTGGGGGATCAACAGCGGATCGTATTG-3′
X, K421A_AS	5′-CATTCTTTTGGCAATACGATCCGCTGTTGATCCC-3′
Y, E62K_S	5′-TCAATATTGCGGGATCTTTGAAAGACCGTACCG-3′
Z, E62K_AS	5′-GCTTTGTCAGCGGTACGGTCTTTCAAAGATCCC-3′

Table S2 Homologous level of CBS-related proteins in *C. elegans*

C. elegans genes are arranged by the level of homology with human CBS. The query sequences are as follows: human CBS (UniProt entry P35520), trypanosomal CBS (UniProt entry Q9BH24) and bacterial CS (UniProt entry P0ABK5). In each group of comparisons, the left-hand column lists the e-value, and the middle and right-hand column list identical and positive matches in percentages respectively. The Table shows three groups of ten CBS homologues in *C. elegans*: ZC373.1 and F54A3.4 have the highest homology with CBS; C17G1.7, R08E5.2, F59A7.9 and K10H10.2 are the most homologous with cysteine synthase; and the remaining homologues belong to other unspecified fold-type II PLP-dependent protein families. AA, number of amino acids in the hypothetical protein; COG, clusters of orthologous groups of proteins; CBS RE, CBS and related enzymes; NA, not assigned; SR, serine racemase.

			Homology [e-value, identities (%), positives (%)]								
Name	AA	COG	human CBS (551 AA)			*T. cruzi* CBS (384 AA)			*E. coli* CS (323 AA)		
ZC373.1	704	CBS RE	8e − 94	54	71	2e − 84	50	66	2e − 30	30	44
F54A3.4	755	CBS RE	4e − 92	54	68	8e − 87	51	66	6e − 27	32	46
C17G1.7	341	NA	2e − 54	44	60	4e − 41	36	51	5e − 62	44	59
K10H10.2	337	CBS RE	4e − 54	38	60	9e − 43	35	56	1e − 60	45	58
R08E5.2	337	CBS RE	1e − 51	37	58	2e − 42	36	55	1e − 57	41	57
F59A7.9	337	CBS RE	7e − 42	36	58	3e − 38	35	54	4e − 56	41	55
F01D4.8	430	CBS RE	2e − 10	24	43	0.012	25	49	0.043	26	46
T25D3.3	427	CBS RE	2e − 09	25	40	0.003	24	44	0.001	28	56
T01H8.2	317	SR	1e − 07	28	43	2e − 04	23	39	0.015	29	48
F13B12.4	435	CBS mRE	5e − 07	21	40	0.037 23	47	5e-04	26	45	

Received 15 August 2011/13 December 2011; accepted 13 January 2012
Published as BJ Immediate Publication 13 January 2012, doi:10.1042/BJ20111478